AFOSR Final Performance Report

Project Title: Biomineralized 3-D Nanoparticle Assemblies with Micro-to-Nanoscale Features and Tailored Chemistries

Award Number: FA9550-05-1-0092

Start Date: Jan. 15, 2005

Program Manager: Dr. Hugh C. De Long

Biomimetics, Biomaterials, and Biointerfacial Sciences
Air Force Office of Scientific Research
Directorate of Chemistry and Life Sciences
875 North Randolph Street

Suite 325, Room 3112
Arlington, Virginia 22203-1768
E-mail: hugh.delong@afosr.af.mil

Phone: (703)696-7722

Fax: (703)696-8449

Principal Investigator: Prof. Ken H. Sandhage
School of Materials Science & Engineering
Institute for Bioengineering and Biosciences
Georgia Institute of Technology
771 Ferst Drive
Atlanta, GA 30332-0245
E-mail: ken.sandhage@mse.gatech.edu
Phone: (404) 894-6882
Fax: (404) 385-6564

Co-Investigator: Prof. Jennifer A. Lewis
Department of Materials Science & Engineering
Faculty Affiliate, Dept. Chemical & Biomolecular Engineering
University of Illinois
Urbana, IL 61801
E-mail: jalewis@ux1.cso.uiuc.edu

Phone: (404) 894-6882
Fax: (404) 894-9140

REPORT DOCUMENTATION PAGE

Form Approved
OMB No. 0704-0188

PLEASE DO NOT RETURN YOUR FORM TO THE ABOVE ORGANIZATION.

1. REPORT DATE *(DD-MM-YYYY)*	2. REPORT TYPE	3. DATES COVERED *(From - To)*
7/1/08	Final Performance Report	January, 2005 to December, 2007

4. TITLE AND SUBTITLE

Biomineralized 3-D Nanoparticle Assemblies with Micro-to-Nanoscale Features and Tailored Chemistries

5a. CONTRACT NUMBER

5b. GRANT NUMBER

FA9550-05-1-0092

5c. PROGRAM ELEMENT NUMBER

6. AUTHOR(S)

Sandhage, Kenneth H.
Lewis, Jennifer A.

5d. PROJECT NUMBER

5e. TASK NUMBER

5f. WORK UNIT NUMBER

7. PERFORMING ORGANIZATION NAME(S) AND ADDRESS(ES)

Georgia Institute of Technology, 505 10th St. NW, Atlanta, GA 30318
University of Illinois, Urbana, IL 61801

8. PERFORMING ORGANIZATION REPORT NUMBER

9. SPONSORING/MONITORING AGENCY NAME(S) AND ADDRESS(ES)

Air Force Office of Scientific Research/NL
801 North Randolph Street
Room 732
Arlington, VA 22203-1977

10. SPONSOR/MONITOR'S ACRONYM(S)

AFOSR

11. SPONSOR/MONITOR'S REPORT NUMBER(S)

AFRL-SR-AR-TR-0562

12. DISTRIBUTION/AVAILABILITY STATEMENT

Please withhold the distribution of this Final Report for 1 year, to allow for complete publication of the discussed results in peer-reviewed journal publications, then Dist A

13. SUPPLEMENTARY NOTES

14. ABSTRACT

This collaborative research project has focused on the integrated use of robust biomimetic or biological silica assembly processes with shape-preserving chemical conversion reactions to produce freestanding 3-D structures with selectable microscale morphologies, nanoscale features, and tailored, non-silica chemistries. Biomimetic 3-D silica structures have been synthesized through Direct-Write Assembly using polyamine-based inks, followed by templated conformal silicification. With proper selection of ink composition and silicification conditions, robust silica structures were formed that retained the patterned morphology after firing to 1000 C. Such 3-D biomimetic silica and biological silica (diatom frustule) structures were converted into freestanding 3-D silica-free replicas comprised of other oxides or metals through the use of gas/solid reactions. For example, these 3-D silica structures were converted into high surface area, microporous Si replicas through reaction with Mg gas (to yield MgO and Si products) and then selective MgO dissolution. Such Si replicas have, in turn, been converted into noble metal replicas through electroless deposition and selective Si dissolution. The reaction kinetics and micro/nanostructural evolution during such reactions have been examined.

15. SUBJECT TERMS

16. SECURITY CLASSIFICATION OF:			17. LIMITATION OF ABSTRACT	18. NUMBER OF PAGES	19a. NAME OF RESPONSIBLE PERSON
a. REPORT	b. ABSTRACT	c. THIS PAGE			19b. TELEPHONE NUMBER *(Include area code)*

Reset

INSTRUCTIONS FOR COMPLETING SF 298

1. REPORT DATE. Full publication date, including day, month, if available. Must cite at least the year and be Year 2000 compliant, e.g. 30-06-1998; xx-06-1998; xx-xx-1998.

2. REPORT TYPE. State the type of report, such as final, technical, interim, memorandum, master's thesis, progress, quarterly, research, special, group study, etc.

3. DATES COVERED. Indicate the time during which the work was performed and the report was written, e.g., Jun 1997 - Jun 1998; 1-10 Jun 1996; May - Nov 1998; Nov 1998.

4. TITLE. Enter title and subtitle with volume number and part number, if applicable. On classified documents, enter the title classification in parentheses.

5a. CONTRACT NUMBER. Enter all contract numbers as they appear in the report, e.g. F33615-86-C-5169.

5b. GRANT NUMBER. Enter all grant numbers as they appear in the report, e.g. AFOSR-82-1234.

5c. PROGRAM ELEMENT NUMBER. Enter all program element numbers as they appear in the report, e.g. 61101A.

5d. PROJECT NUMBER. Enter all project numbers as they appear in the report, e.g. 1F665702D1257; ILIR.

5e. TASK NUMBER. Enter all task numbers as they appear in the report, e.g. 05; RF0330201; T4112.

5f. WORK UNIT NUMBER. Enter all work unit numbers as they appear in the report, e.g. 001; AFAPL30480105.

6. AUTHOR(S). Enter name(s) of person(s) responsible for writing the report, performing the research, or credited with the content of the report. The form of entry is the last name, first name, middle initial, and additional qualifiers separated by commas, e.g. Smith, Richard, J, Jr.

7. PERFORMING ORGANIZATION NAME(S) AND ADDRESS(ES). Self-explanatory.

8. PERFORMING ORGANIZATION REPORT NUMBER. Enter all unique alphanumeric report numbers assigned by the performing organization, e.g. BRL-1234; AFWL-TR-85-4017-Vol-21-PT-2.

9. SPONSORING/MONITORING AGENCY NAME(S) AND ADDRESS(ES). Enter the name and address of the organization(s) financially responsible for and monitoring the work.

10. SPONSOR/MONITOR'S ACRONYM(S). Enter, if available, e.g. BRL, ARDEC, NADC.

11. SPONSOR/MONITOR'S REPORT NUMBER(S). Enter report number as assigned by the sponsoring/ monitoring agency, if available, e.g. BRL-TR-829; -215.

12. DISTRIBUTION/AVAILABILITY STATEMENT. Use agency-mandated availability statements to indicate the public availability or distribution limitations of the report. If additional limitations/ restrictions or special markings are indicated, follow agency authorization procedures, e.g. RD/FRD, PROPIN, ITAR, etc. Include copyright information.

13. SUPPLEMENTARY NOTES. Enter information not included elsewhere such as: prepared in cooperation with; translation of; report supersedes; old edition number, etc.

14. ABSTRACT. A brief (approximately 200 words) factual summary of the most significant information.

15. SUBJECT TERMS. Key words or phrases identifying major concepts in the report.

16. SECURITY CLASSIFICATION. Enter security classification in accordance with security classification regulations, e.g. U, C, S, etc. If this form contains classified information, stamp classification level on the top and bottom of this page.

17. LIMITATION OF ABSTRACT. This block must be completed to assign a distribution limitation to the abstract. Enter UU (Unclassified Unlimited) or SAR (Same as Report). An entry in this block is necessary if the abstract is to be limited.

Accomplishments/New Findings:

· Biomimetic 3-D silica structures with controlled microscale features have been synthesized through Direct-Write Assembly using PAH/PAA inks, followed by templated conformal silicification. With proper selection of ink composition and silicification conditions, robust silica structures were formed that retained the patterned morphology after firing to 1000^{o}C.

· A new strategy for enhancing the silicification kinetics of patterned PAH/PAA scaffolds was developed. This approach, which relies on pre-etching the scaffolds via oxygen plasma treatment prior to their exposure to silicic acid, leads to nearly an order of magnitude increase in silicification rates.

· DWA-derived silicified woodpile structures have been converted into $TiOF_2$ via a low-temperature metathetic reaction, and then into TiO_2 via a water vapor de-fluorination treatment. Under proper reaction conditions, warping of the structures was avoided, so that nano-crystalline TiO_2 replicas could be produced with excellent preservation of microscale features.

· Bio-organic templates have been converted into titania replicas. SiO_2 replicas of pollen particles were prepared by infiltration with silicic acid and then firing (S.R. Hall, Univ. Bristol). The silicified replicas were converted into TiO_2 by reaction with TiF_4(g) and then with H_2O(g). The pollen shape and fine nanoscale protuberances on the pollen surface were well preserved after conversion. This hybrid approach may be applied to a variety of bio-organic templates, which are more common in nature than bio-inorganic structures.

· SiO_2-based diatom frustules were converted, via a low-temperature magnesiothermic reduction process, into nanocrystalline Si replicas with high surface areas (>500 m^2/g) and with significant microporosity ($\leq$ 2 nm dia.). These 3-D Si frustule replicas were found to be rapid, low voltage, minimally-invasive sensors of NO(g) and to exhibit photoluminescence. The kinetics of magnesiothermic reaction of Stober SiO_2 microspheres and diatom frustules into MgO-bearing replicas have been evaluated with high temperature x-ray diffraction analyses.

· Porous Si replicas of diatom frustules were, in turn, converted into freestanding (Si-free) porous, noble metal (Ag, Au, or Pd) nanoparticle replicas. Brief immersion in electroless plating solutions resulted in complete penetration and deposition of an interconnected network of metal nanoparticles on the Si nanoparticle surfaces throughout the porous walls of the Si replicas. Subsequent selective dissolution of the Si then yielded a porous, interconnected network of nanocrystalline Ag, Au, or Pd that retained the 3-D morphology of the starting frustules. This process provides a means of synthesizing porous metal nanoparticle assemblies with tailored 3-D shapes for catalytic, filtration, sensor, electrical, and thermal applications.

· SiC replicas of diatom frustules were synthesized via deposition of C onto Si frustule replicas (produced by magnesiothermic reduction of SiO_2 frustules) and then high temperature reaction of the C and underlying Si. This approach enables, for the first time, the syntheses of porous SiC particles with a wide variety of selectable 3-D shapes and aspect ratios for use as strong, oxidation-resistant reinforcements in composites.

· Carbon replicas of diatom frustules were formed via selective removal of Si from SiC frustule replicas by reaction with Cl_2(g). The C replicas possessed very high surface areas (1370 m^2/g) and contained a significant population of open micropores ($\leq$ 2 nm dia.). Carbon particles with such ultrahigh surface areas and open, hollow, and selectable 3-D shapes are highly attractive for catalysis, filtration, and stiff, lightweight reinforcements for composites.

Summary:

Three-dimensional (3-D) microperiodic polymer templates that mimic the silica microshells (frustules) of diatoms in both size and shape have been synthesized via direct-write assembly (DWA) of concentrated polyamine-based inks. The conversion of these templates into silica-organic hybrid structures via biomimetic silicification has been demonstrated. The effects of two key parameters, the polyamine content and molecular weight, on this process have been explored. A novel pathway to enhance the mineralization kinetics, through plasma etching of the initial polymeric template, has been devised.

DWA-biosculpted 3-D filamentary silica structures have been converted into titania replicas via a two-step process: i) formation of $TiOF_2(s)$ via reaction with $TiF_4(g)$ and then ii) conversion of $TiOF_2(s)$ into $TiO_2(s)$ via reaction with water vapor. The second process was initially conducted with the use of oxygen as the carrier gas for water vapor (i.e., $H_2O(g)$ was carried to the silica structures by passing $O_2(g)$ through a heated water bath). This oxidizing treatment resulted in detectable shrinkage (on the order of 10% linear shrinkage) and significant warping (curling) of the filamentary titania replicas. The shrinkage and warping were significantly reduced by replacing the oxygen with argon as the carrier gas in the second process. Structural and chemical analyses (via electron microscopy, energy dispersive x-ray analysis, and selected area electron diffraction analysis) confirmed that such chemical conversion could be completed at modest temperatures ($\leq 300^oC$) with a preservation of shape and fine features and without microcracking. Optical reflectivity measurements of the silicified and reacted specimens indicated that the periodicity of the woodpile structures was preserved upon reactive conversion of the silica.

A collaboration between the Sandhage and Hall (Chemistry Dept., University of Bristol) has demonstrated how bio-organic structures may be converted into functional nanocrystalline inorganic replicas. Silicified replicas of pollen particles were prepared by infiltration with silicic acid and then slow heating to 600^oC (S. R. Hall, Chemistry Dept., Univ. Bristol). The silicified pollen replicas were then converted into TiO_2 replicas by exposure to $TiF_4(g)$ at 210^oC-300^oC and then to water vapor at 300^oC. While the general pollen shape was preserved after reaction at 210^oC-300^oC, the fine nanoscale protuberances on the pollen surface were particularly well preserved after the lower temperature (210^oC) treatment. This hybrid (template infiltration, firing, and then reactive gas/solid conversion) approach may be applied to a wide variety of bio-organic templates, which are much more common in nature than bio-inorganic structures.

Dynamic high temperature x-ray diffraction analysis have been conducted, with the aid of a closed, heated, x-ray transparent graphite reaction chamber, to evaluate the rate of conversion of silica spheres and diatom frustules into MgO-bearing replicas. A magnesium gas source was sealed along with SiO_2 specimens (amorphous spheres of uniform diameter, or diatom frustules) inside the graphite chamber. The chamber was then heated to a temperature in the range of 625-825^oC to allow for the generation of magnesium vapor in the vicinity of the silica specimens. Incident and diffracted Mo Kα x-rays were passed through the sidewalls of the closed graphite chamber to allow for detection of MgO formation. The MgO formation kinetics were found to obey the Carter model for the conversion of solid reactant spheres into solid product spheres of larger volume. The Carter rate constants obtained from reaction experiments with silica spheres were used to predict the times required for the complete reaction of diatom frustules. The predicted times were consistent with independent frustule reaction experiments.

Silica-based diatom frustules have been converted into nanocrystalline, microporous Si replicas through the use of low-temperature magnesiothermic reduction. Silicon replicas of were

synthesized by: i) reaction with Mg(g) at 650°C to yield co-continuous MgO + Si replicas and then ii) selective dissolution of the MgO to yield microporous Si replicas. The Si replicas retained frustule features as fine as a few tens of nm is size. The replicas possessed high surface areas (>500 m^2/g), a significant population of micropores, and average crystallite sizes as fine as 8 nm. Microporous silicon frustule replicas were produced that exhibited red photoluminescence upon irradiation with 275 nm light. This bio-enabled approach is an attractive means of synthesizing 3-D assemblies of microporous Si nanoparticles ("Bio-Si MEMS") with a wide variety of controlled, hierarchical morphologies.

Nanocrystalline silicon carbide replicas of silica-based diatom frustules have been synthesized through a series of reactions. The silica frustules were first converted into porous silicon replicas through the use of a modest temperature magnesiothermic conversion process developed previously in this project. The porous silicon replicas were then coated with carbon via exposure to a flowing methane/argon atmosphere at 950°C for 2.5 h. The carbon coating was then allowed to react with the underlying silicon at 1200°C for 12 h to form SiC. X-ray diffraction and electron diffraction analyses confirmed that the conversion into SiC was completed under these relatively modest firing conditions. The SiC-converted structures retained the morphologies of the starting diatom frustules. This approach enables, for the first time, the syntheses of porous SiC particles with a wide variety of selectable 3-D shapes and aspect ratios for use as strong, lightweight reinforcements in polymer-matrix, metal-matrix, and ceramic-matrix composites.

Carbon replicas of diatom frustules with ultra high surface areas have also been generated. The silicon carbide frustule replicas described above were exposed to a flowing chlorine gas stream at 950°C for 3 h. The silicon within the silicon carbide reacted selectively with the chlorine to form silicon tetrachloride gas that then migrated away from the frustule replicas to yield porous carbon replicas. Energy dispersive x-ray analyses and electron diffraction analyses of cross-sections of the carbon-converted frustules confirmed that the silicon could be completely removed within 3 h of exposure to chlorine at 950°C to yield amorphous carbon replicas. The carbon replicas retained the shapes and fine features of, but possessed much higher surface areas than, the starting diatom frustules. Analyses of nitrogen adsorption/desorption curves yielded a BET surface area of 1370 m^2/g for the carbon replicas (compared to a surface area of only a few m^2/g for the starting diatom frustules). Such analyses also indicated that the carbon frustule replicas contained a significant population of open micropores ($\leq$ 2 nm dia.); that is, 22% of the total volume of pores < 36 nm in size was associated with micropores. The ability to form carbon particles with such ultrahigh surface areas and with open, hollow, and selectable shapes is highly attractive for applications in catalysis and filtration, and for the syntheses of stiff reinforcements for lightweight composites.

The silicon frustule replicas have also been used as templates for conversion into silver, gold, or palladium replicas. The replicas were immersed in a given electroless solution for only 1 min to allow for the infiltration of the solution into, and deposition of Ag, Au, or Pd throughout, the porous silicon structures. Selective dissolution of the silicon then yielded freestanding Ag, Au, or Pd replicas. This scalable conversion process may be used to generate a variety of porous metal replicas of biologically- or synthetically-derived silica templates with a wide range of 3-D morphologies for use in catalysis, filtration, sensor, electrical, and thermal applications.

Biomimetic Silicification of 3-D Polyamine-rich Scaffolds Assembled by Direct Writing
(co-PI Jennifer A. Lewis, University of Illinois, Urbana, IL)

Objective: To create 3-D micro-periodic polymer templates for biomimetic silicification via direct-write assembly and explore their conversion into silica-organic hybrid structures with diatom-like motifs.

Direct writing of concentrated polyelectrolyte inks, a process akin to spinning spider webs, enables the assembly of micro-patterned structures that emulate the stunning shapes exhibited by diatoms (see Figure 1). To convert these organic structures into the desired inorganic-organic hybrids, we have exploited the recent discovery that, in addition to natural silaffin peptides and long-chain polyamines, several synthetic amino acids, peptides and polyamines also hydrolyze and condense silica precursors under ambient conditions. Central to our approach is the creation of a synthetic polyamine-rich ink capable of being patterned by direct writing and, subsequently, converted to diatom-like structures via biomimetic silicification. Although other methods such as block polypeptide templating and holographic patterning offer the possibility of rational design, they are presently incapable of mimicking the structural complexity associated with natural diatoms. The precise molecular mechanisms that give rise to thousands of variations in their intricately patterned siliceous cell walls are poorly understood. While a simple, yet elegant model involving repeated phase separation events within silica deposition vesicles has been postulated, this level of sophistication is beyond the reach of current synthetic self assembly methods. By decoupling the patterning process from silica morphogenesis, we have recently demonstrated the directed assembly of 3-D synthetic diatom frustules.

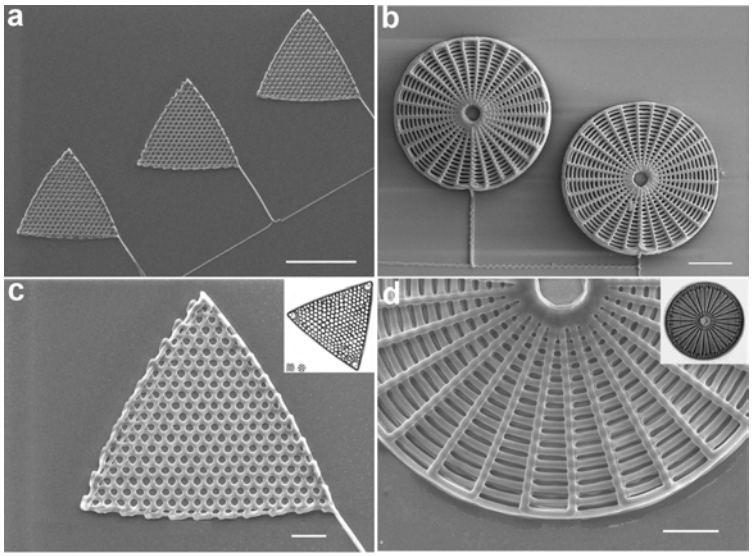

Figure 1. a, Triangular- and **b**, web-shaped polyamine-rich scaffolds (scale bars: 100 μm and 50 μm, respectively). Higher magnification views **c** and **d** (scale bars: 20 μm). [Inset: Natural diatoms **c**, *Triceratium favus ehrenberg* and **d**, *Arachnoidiscus ehrenberg*.]

To highlight the shape complexity achievable by direct-write assembly, two polymer scaffolds have been patterned in the form of naturally occurring diatoms, *Triceratium favus ehrenberg* (a triangular-shaped structure) and *Arachnoidiscus ehrenberg* (a web-shaped structure), in both their overall dimensions (~ 100-200 μm in size) and their finer-scale detail (see Figure 1) via patterning a polyamine-rich ink. The subsequent biomimetic silicification of these 3-D polymeric scaffolds to produce synthetic diatoms must satisfy two important requirements. First, the templating process must preserve their intricately patterned features. This poses a significant challenge, since the structural integrity of these polyelectrolyte-based scaffolds depends strongly on pH and ionic strength. Second, silica condensation must occur uniformly throughout the scaffolds to yield the desired inorganic-organic hybrids. We have recently identified an optimal protocol for their silicification, in which the polymer scaffolds are

first heated to 180°C to induce partial cross-linking between the PAH and PAA chains through amide bond formation. This treatment enhanced their structural integrity allowing them to remain intact even after several days of immersion in a phosphate-buffered, silicic acid solution. Following this process, the preheated scaffolds were immersed sequentially into a silicic acid solution (50 mM, pH 3) for 48 h to promote silica condensation followed by immersion in 3.5 ml of phosphate-buffer solution (30 mM, pH 8) for 0.5 h to further promote silica formation and then subsequently rinsed thoroughly with deionized water. This approach is shape preserving, resulting in silica condensation at the scaffold surface, as evidenced by nanoparticle formation (see Fig. 2). The total silica yield determined by thermogravimetric analysis was 52 wt%, which confirmed that significant mineralization had occurred.

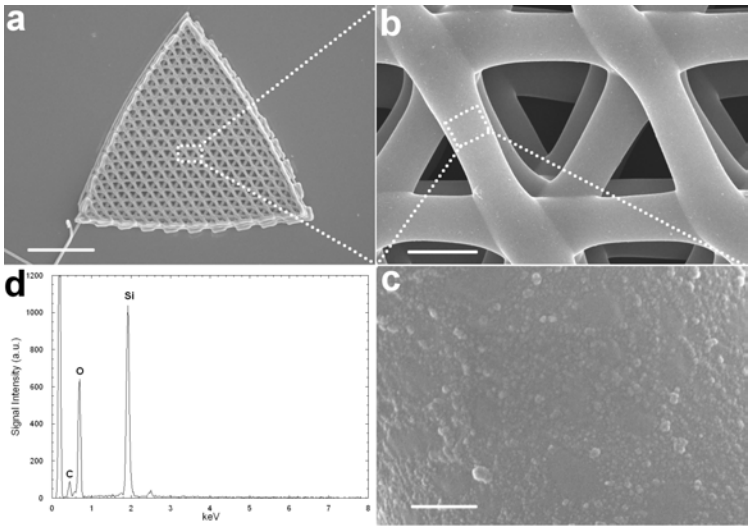

Figure 2. Sequential zoom-in image series, **a** – **c**, final scale surface morphology of structure after sequential immersion protocol. Scale bars (**a**) 50 μm, (**b**) 3 μm, (**c**) 250 nm. **d**, Energy dispersive X-ray spectrum.

Optimizing Biomimetic Silicification (co-PI Jennifer A. Lewis)

The biomimetic silicification process depends strongly on the ink composition, silicification pH, and silicification protocol. Although other polyelectrolyte inks, such as a PAA-rich ink, can be patterned by direct-write assembly, these 3D scaffolds do not catalyze the precipitation of silica like their PAH-rich counterparts (see Figure 3). Moreover, the silica content of the silicified scaffolds also depends on the amount of excess polyamine present to participate in the mineralization process (see Figure 4). For example, scaffolds produced from polyelectrolyte inks with 1:1 stoichiometric charge group ratio exhibited low silica content (10 wt%) after the silicification process. However, once this charge group ratio was two or higher, significant silica formation occurred independent of polyamine molecular weight. The extent of biomimetic silicification of these polyamine-rich scaffolds varied with the silicification pH. We found that the optimal pH for highest silica content was between pH 3 and 4.

By tailoring the ink composition, silicification pH and silicification protocol, we have identified an optimized protocol for the biomimetic silicification of polyamine-rich scaffolds. These robust structures were able to withstand heat treatment to 1000^{o}C (complete polymer removal) without cracking.

The biomimetic silicification kinetics depend on the morphology of the polyamine-rich matrices. To investigate this effect, oxygen plasma etching was used to expose the underlying porous polymer matrices. Figure 5 depicts the changes in morphology induced upon etching. Prior to etching, the as-patterned, partially cross-linked filaments have a smooth surface morphology. After a short etching time (30 s), small islands approximately 70 to 100 nm in size were observed on the filament surface, which may have arisen due to preferential etching of

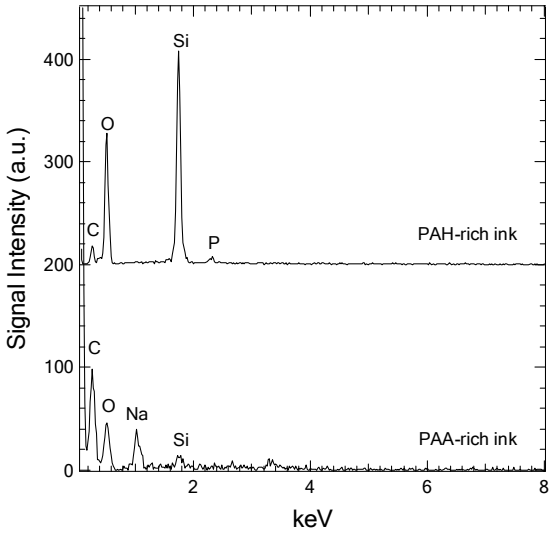

Figure 3. EDX spectra from scaffolds of PAH-rich ink and PAA-rich ink after silicification.

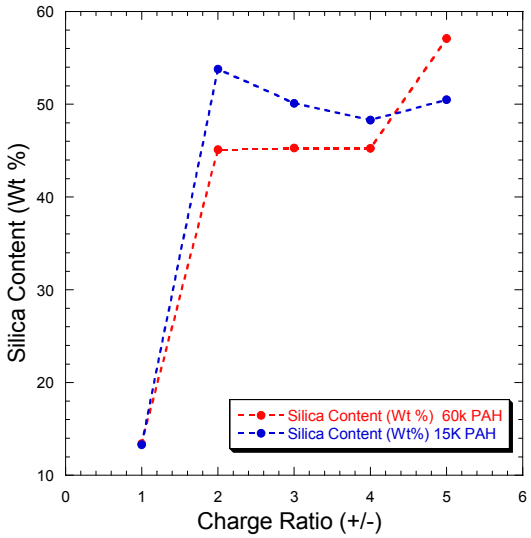

Figure 4. Effects of molecular weight and charge group ratio on the silicification process.

regions of low amide cross-link density. Upon complete removal of the surface layer, their underlying porous morphology was revealed. After further plasma etching, the voids grew in size and underwent some surface roughening. The dense outer surface and internal voids observed for PAH-rich filaments coagulated in alcohol-rich reservoirs were analogous to features found in asymmetric membranes, which undergo phase inversion during their formation. Under poor solvent conditions, a homogeneous polymer solution phase separates into a polymer-rich matrix and a polymer-poor fluid, the latter of which gives rise to internal voids upon drying. A dense outer layer (or skin) forms because rapid gelation at the filament-reservoir interface inhibits phase separation. Hence, we can tune both the filament roughness and specific surface area by controlling their coagulation as well as post-etching conditions.

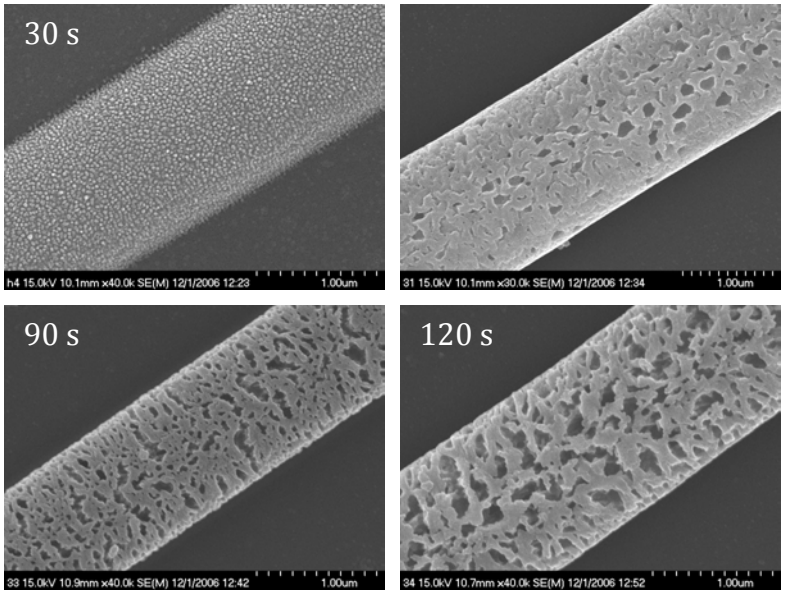

Figure 5. SEM images of PAH-PAA filaments printed by DIW upon exposure to oxygen plasma etching for various times.

The porous nature of the etched PAH-PAA filaments and corresponding films greatly enhanced the silicification kinetics. To demonstrate this, we first exposed PAH-PAA films with 2:1 charge group ratio to oxygen plasma for 45 s prior to sequential silicification process. As determined by surface profilometry, an approximately 250 nm thick polymer layer was removed under the conditions employed. After exposure to silicic acid, its silica content experienced a rapidly increase to ~45 wt% within the first 5 h (see Figure 6), which represented nearly an order of magnitude decrease in silicification time relative to the original films. We attribute our observation of enhanced silicification kinetics to the removal of the dense surface layer by oxygen plasma ablation, which thereby exposed the underlying microporous polymer matrix.

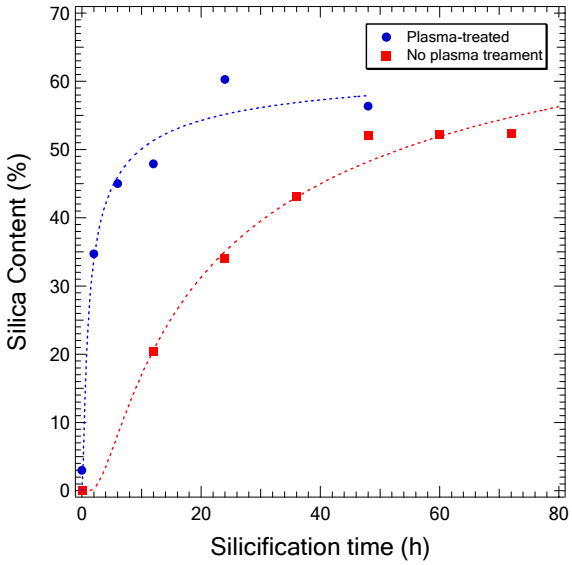

Figure 6. Silica content as a function of silicification time for plasma-treated (45 s ●) and untreated (■) PAH-PAA films subjected to the sequential immersion method. Dotted lines are fitted curves according to *Eq 3.5* to estimate the diffusion coefficients of silicic acids in the polymer network.

<u>Direct Writing of Photonic Crystals</u> (co-PI Jennifer A. Lewis)

Direct ink writing (DIW) offers a facile approach for creating 3D woodpile structures (see Figure 7) for photonic band gap applications. This structure, first introduced by Ho, Chan, and Soukoulis[1,2], is composed of dielectric rods stacked in a periodic array such that their contact points form a diamond-like lattice. It consists of layers of one-dimensional rods with a stacking sequence that repeats itself every four layers with a repeat distance of *c*. Within each layer, the axes of the rods are parallel to each other with a pitch of *d*. Between adjacent layers, the rod orientation is rotated by 90°. The position of rods is shifted by *d/2* between every other layer. For a special case, when $c/d = \sqrt{2}$, the structure adopts a face-centered-cubic (f.c.c.) primitive unit cell[2] with a basis of two rods. Otherwise, the lattice symmetry is face-centered-tetragonal (f.c.t.).

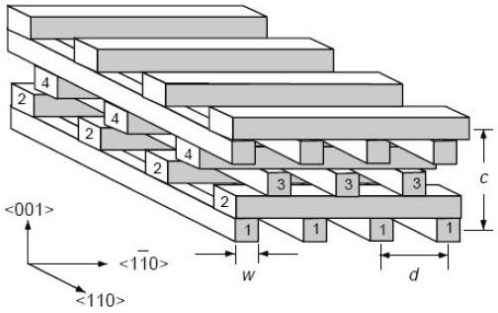

Figure 7. Diagram of layer-by-layer woodpile photonic crystal. It consists of layers of one-dimensional rods with a stacking sequence that repeats itself every four layers. An unit cell is composed of 4 layers with repeating distance *c* and in-plane pitch distance *d*.

By tailoring the ink composition, silicification conditions, as well as printing conditions, we have identified an optimized protocol for assembling high quality polymer woodpile structures and their subsequent biomimetic silicification to produce silica woodpile structures (see Fig. 8). Figure 9 shows the reflectance spectrum from the polymer template (RW = 4 μm). The peak near 5.5 μm corresponds to the first stop band and has a maximum reflectance of 0.4. This value represents a two-fold improvement over prior polymer woodpile structures created by using direct ink writing, demonstrating that high-quality templates can be produced by using this

approach. The presence of well-defined optical features around 2.5 μm is also remarkable, since optical features at shorter wavelengths are suppressed by structural inhomogeneities.

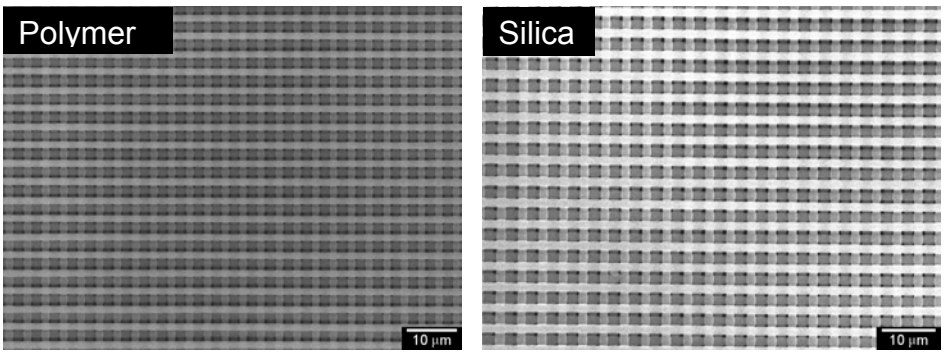

Figure 8. (a) Polyamine-rich woodpile structure before silicification, and (b) silicified woodpile structure.

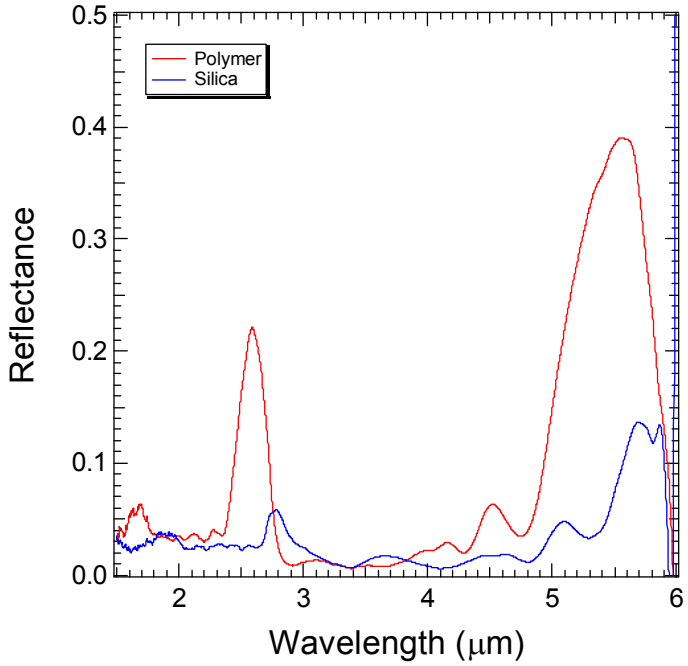

Figure 9. Optical reflectance collected along the perpendicular direction of woodpile sample before and after silicification.

Chemical Conversion of DWA-derived Silica Structures into Titania Replicas

(J. A. Lewis Group, University of Illinois and K. H. Sandhage Group, Georgia Tech)

The low-temperature, shape-preserving reactive conversion of silicified structures, with 3-D shapes generated via direct write assembly of polyamine-rich scaffolds, is a versatile hybrid (biomimetic/synthetic) approach for synthesizing functional, nanocrystalline microcomponents. Collaborative work (Lewis, Sandhage groups) in this project has resulted in the synthesis and reactive conversion of DWA-patterned silica-bearing structures into titania replicas.

A secondary electron image of a direct-write-assembled and silicified lattice structure is shown in Figure 10a below. This SiO_2-based structure was exposed to TiF_4(g) (within an argon

atmosphere) at 210°C for 8 h to allow for conversion into $TiOF_2$(s) (as per the metathetic displacement reaction (1a) below) and then to a flowing stream of H_2O(g) in Ar at 350°C for 6 h to selectively remove the fluorine and thereby generate TiO_2 (as per the reaction (1b) below).[3,4]

$$SiO_2(s) + 2TiF_4(g) \Rightarrow 2TiOF_2(s) + SiF_4(g) \quad (1a)$$

$$TiOF_2(s) + H_2O(g) \Rightarrow TiO_2(s) + 2HF(g) \quad (1b)$$

Secondary electron images of the silicified structure from Figure 10a after such reactive conversion into TiO_2 is shown in Figures 10b-d. The lattice morphology was well-preserved upon conversion into titania. As seen in the higher magnification images in Figures 10c and d, the converted filaments were free of microcracks and were comprised of nanocrystals. In order to confirm that the reaction was completed, cross-sections of converted filaments were prepared using focused ion beam milling. A secondary electron image and corresponding x-ray maps (for titanium, oxygen, carbon, and platinum) of a converted filament cross-section are shown in Figure 11. The x-ray maps revealed the presence of titanium and oxygen throughout the filament cross-sections, along with some residual carbon (from the original polyamines in the direct-write-assembled template). (Note: the platinum seen in Figures 11a and 11e was deposited just prior to focused ion beam milling.) EDX analyses indicated that the silicon had been completely removed from the filaments during the course of reaction at 210°C.

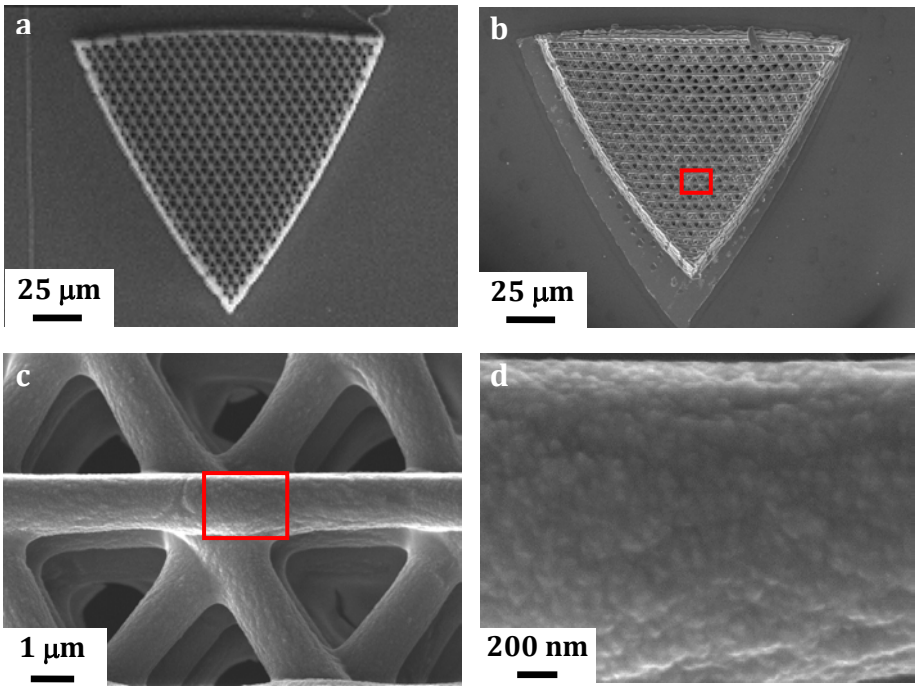

Figure 10. (a) Secondary electron image of a direct write assembled, silicified triangular lattice structure, (b-d) the same structure after reactive conversion into TiO_2 via reactions (1a) and (1b).

The reactive conversion of face-centered-cubic silicified woodpile structures (with 12 layers of filament stacking) has also been examined. Such structures have been reacted with TiF_4(g) (within an argon atmosphere) at 220°C for 12 h to yield $TiOF_2$ replicas. The reflectance spectra of silicified and $TiOF_2$-converted woodpile replicas are shown in Figures 12a and b, respectively. The reflectance peaks in the 7-8 μm and 9-10 μm ranges generated by the silicified woodpile

structures were also generated by the $TiOF_2$-converted replicas, which provided further confirmation that the periodicity of the woodpile structure was preserved upon such conversion.

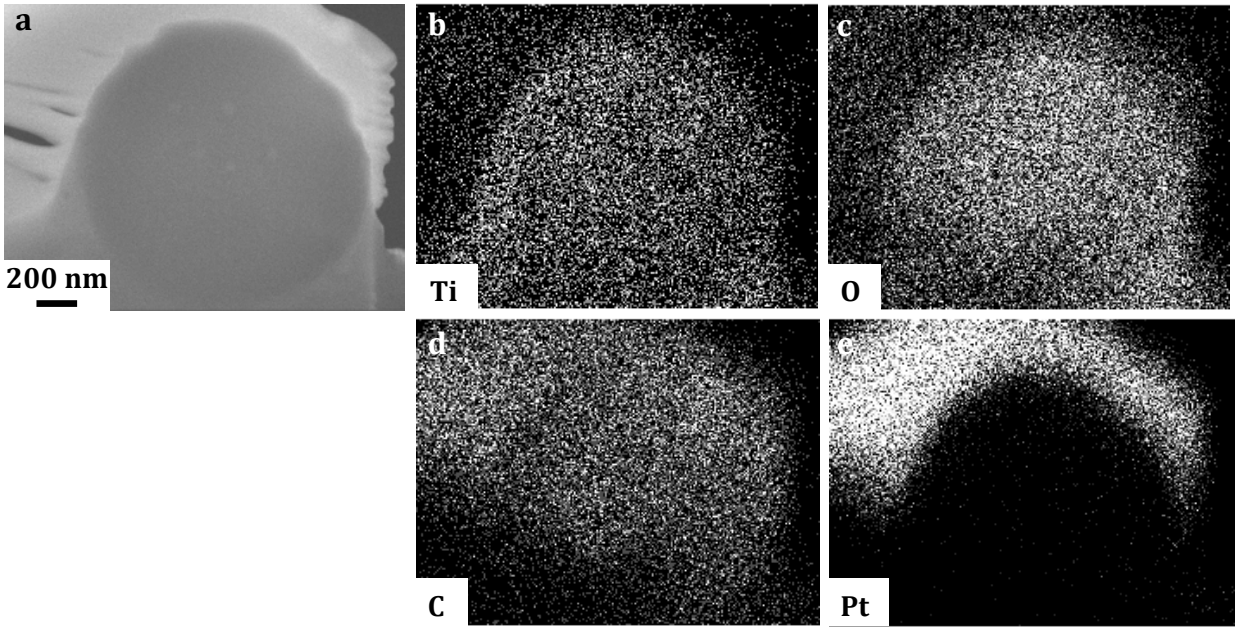

Figure 11. (a) Secondary electron image (b-e) corresponding x-ray maps for titanium, oxygen, carbon, and platinum, respectively, of a cross-section of a silicified filament after reactive conversion into titania.

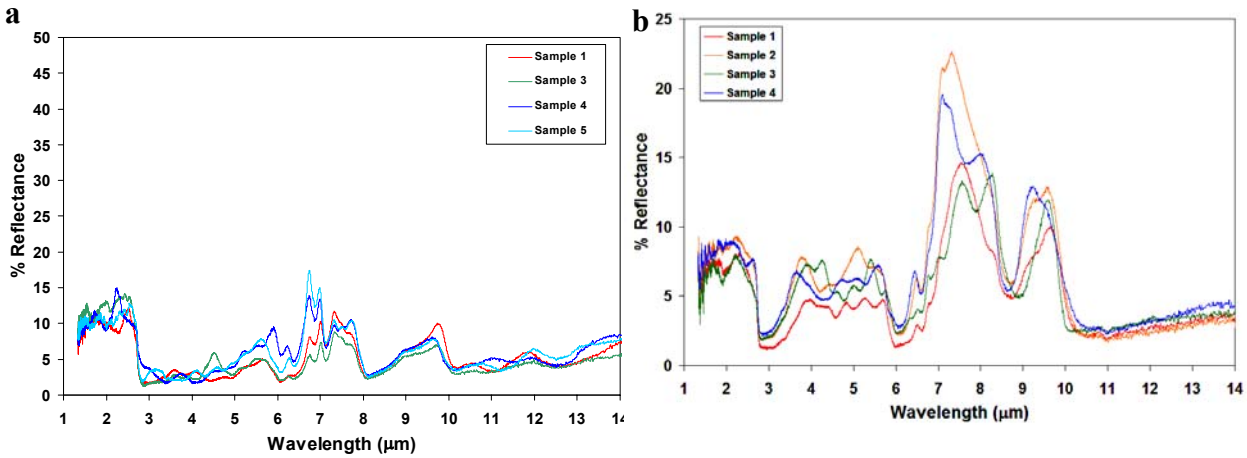

Figure 12. Optical reflectivity spectra of: (a) a silicified woodpile structure and (b) the woodpile structure after conversion into a $TiOF_2$ replica via reaction with TiF_4(g) at 220°

Chemical Conversion of Biotemplated Silica into Titania Replicas

(K. H. Sandhage Group, Georgia Tech, in collaboration with Simon Hall, University of Bristol)

Over the past year, collaborative work has been conducted with Dr. Simon Hall (Chemistry Dept., University of Bristol) to evaluate the syntheses of titania structures with morphologies generated from bioorganic structures, which are generally more prevalent in nature than bioinorganic structures. The Hall group synthesized silica replicas of pollen by soaking the

pollen in a silicic acid solution, and then heating slowly in air to 600°C to convert the silicic acid into an interconnected silica structure.[5] Secondary electron images and EDX analysis of the silica-bearing pollen replicas are shown in Figure 13. The surfaces of the silica pollen replicas retained nanoscale protuberances inherited from the native pollen.

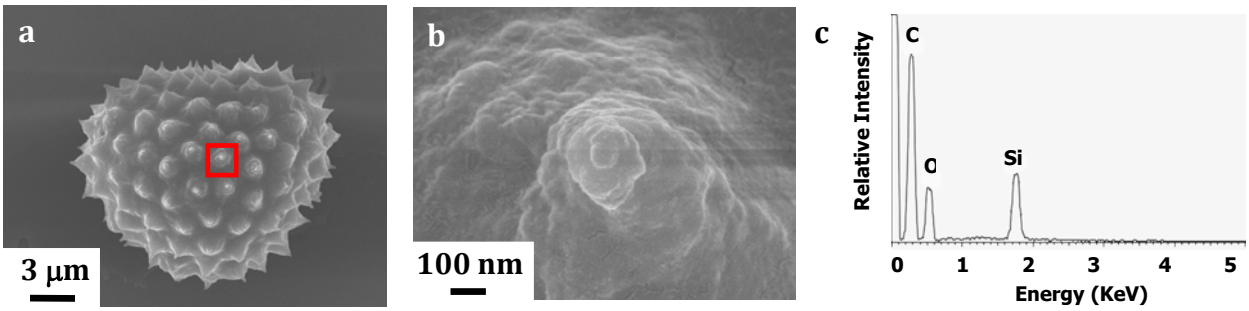

Figure 13. (a,b) Secondary images of SiO_2 replicas of pollen. (c) EDX analysis of the silica pollen replica.

These microscale, nanostructured silica pollen replicas were then converted into titania replicas using the two-stage reaction process described above (i.e., reaction with $TiF_4(g)$ to form $TiOF_2$ and then with $H_2O(g)$ to generate TiO_2). The initial $TiF_4(g)$ reaction step was conducted at temperatures/times ranging from 210°C/12 h to 300°C/5 h in order to evaluate which reaction conditions would lead to the best preservation of shape and nanoscale features of the silica pollen structures (note: the second $H_2O(g)$ treatment for fluorine removal and titania formation was maintained at 300°C for 12 h). Secondary electron images of the resulting structures are shown in Figure 14. The images in Figures 14a-c were obtained with the use of an initial $TiF_4(g)$

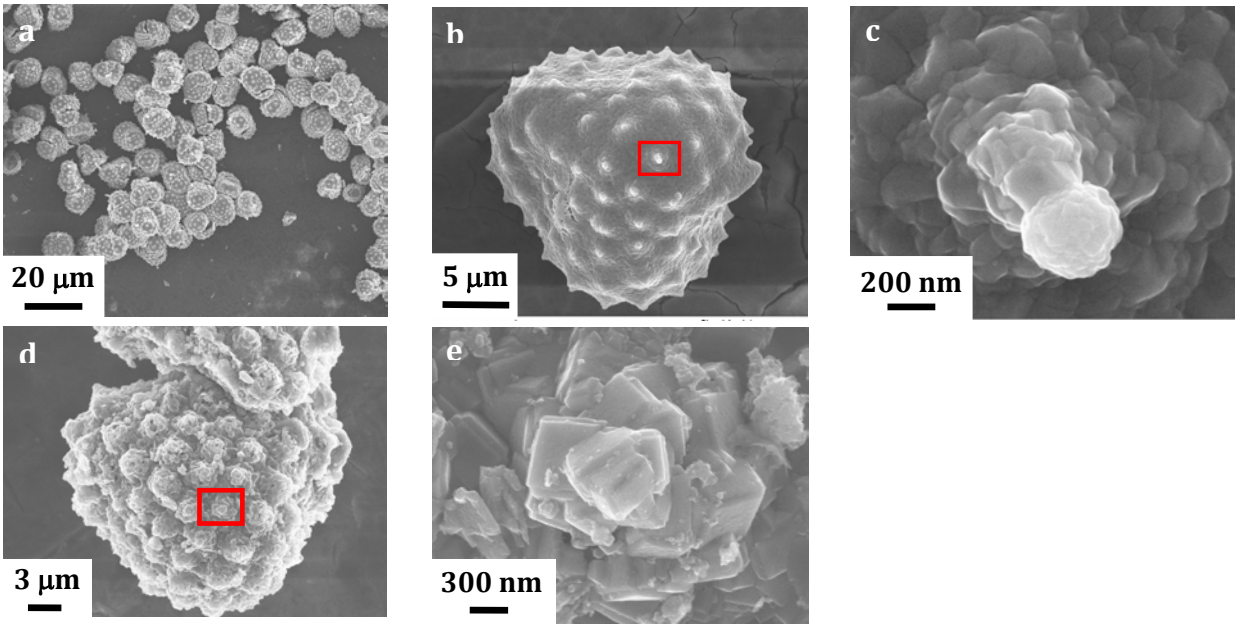

Figure 14. Secondary images of titania-converted silica pollen replicas. The images in (a)-(c) were obtained from specimens exposed to $TiF_4(g)$ at 210°C for 12 h, followed by exposure to $H_2O(g)$ at 300°C for 12 h. The images in (d) and (e) were obtained from specimens exposed to $TiF_4(g)$ at 300°C for 5 h, followed by exposure to $H_2O(g)$ at 300°C for 12 h.

reaction treatment at 210°C/12 h, whereas the images in Figures 14d and 14e were obtained using the 300°C/5 h treatment. While the general shapes of the silica pollen replicas were preserved for both types of TiF_4(g) reaction treatments, the titania crystals produced by the 210°C/12 h treatment were finer (compare Figures 14c and 14e) and, as a result, the nanoscale features of the protuberances were more precisely retained with this treatment (note: prior work with diatom frustules has also shown that the use of such lower temperature/longer time TiF_4(g) reaction treatments yielded finer grain, more precise titania replicas). The absence of detectable Si by EDX analysis (Figure 15a) and the detection of only anatase peaks in the x-ray diffraction pattern (Figure 15b) confirmed that the 210°C/12 h TiF_4(g) treatment followed by the 300°C/12 h H_2O(g) treatment resulted in complete conversion of the silica pollen replicas into anatase TiO_2.

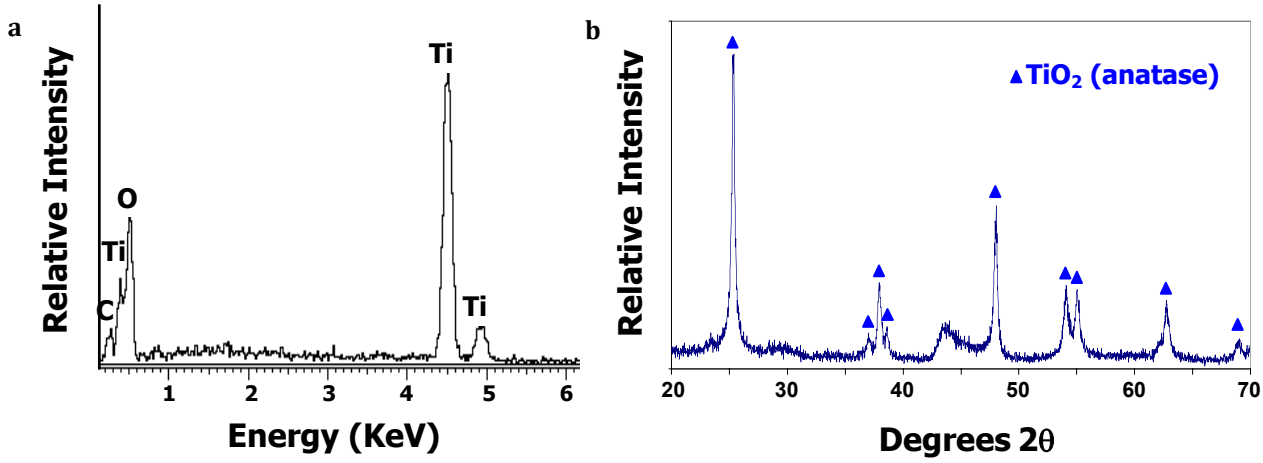

Figure 15. (a) EDX analysis and (b) XRD analysis of titania-converted pollen replicas produced by exposure of silica pollen replicas to TiF_4(g) at 210°C for 12 h, followed by exposure to H_2O(g) at 300°C for 12 h. (Note: the broad peak located near 44 degrees was generated by the specimen holder.)

Chemical Conversion of Si Replicas of Diatom Frustules into SiC Replicas

(K. H. Sandhage Group, Georgia Tech)

Silicon carbide (SiC) is a covalently-bonded ceramic compound with excellent oxidation resistance and high thermal conductivity, hardness, and strength. These properties make silicon carbide an attractive reinforcement phase in polymer-matrix, metal-matrix, and ceramic-matrix composites. The morphologies (shape, aspect ratio, porosity) of SiC reinforcement particles can strongly influence the mechanical behavior of such composites. For example, the infiltration of a fluid polymer, metal, or glass matrix into porous SiC particles can result in good mechanical interlocking of the particles with the solidified matrix and, hence, good load transfer to the SiC particles. Aspected SiC particles dispersed throughout a ceramic matrix composite can also lead to enhanced toughening due to crack deflection. However, the ability to synthesize SiC particles with well-controlled and selectable 3-D shapes, aspect ratios, and porosities has not been possible via conventional ceramic powder processing.

Published work supported by this AFOSR project has demonstrated that silica-based diatom frustules can be converted into silicon replicas via a magnesiothermic reduction process involving the following reaction[6]:

$$2Mg(g) + SiO_2(s) \Rightarrow 2MgO(s) + Si(s) \quad (2)$$

Because the two product phases of this reaction, MgO and Si, are present at volume fractions in excess of the percolation limit for each phase (i.e., 2 moles of MgO and 1 mole of Si correspond to 65.1 vol% MgO and 34.9 vol% Si), the selective dissolution of MgO in hydrochloric acid yields a silicon replica of the starting silica diatom frustule. Furthermore, because the molar volume of Si (12.06 cm^3/mole[7]) is 53.2-58.4% less than that for SiO_2 (25.8 cm^3/mole for cristobalite, 29.0 cm^3/mole for amorphous silica[7,8]), the silicon replica was substantially more porous than the starting silica frustule. The conversion of such porous Si frustule templates into SiC replicas via a two-step reaction process has been examined. In the first step, the silicon frustule replicas were exposed to a flowing 10% CH_4/90% Ar gas mixture at 950°C for 2.5 h to allow for the deposition of carbon on the exposed frustule surfaces. In the second step, the carbon-coated frustules were heated in an argon atmosphere to 1200°C for 12 h, to allow for the reaction of the carbon coating with the underlying silicon to yield silicon carbide. While the conventional synthesis of SiC is often conducted at much higher temperatures, a modest reaction temperature of 1200°C was selected to avoid distortion of the frustule morphology due to grain coarsening during reaction or due to creep of the silicon (the melting point of silicon is 1410°C). X-ray diffraction analyses at various stages of reaction are shown in Figure 16. The absence of silicon peaks in Figure 16c indicated that the 1200°C treatment resulted in complete conversion of the silicon into silicon carbide. The SiC diffraction peaks were quite broad. Application of the Scherrer equation indicated that the average SiC crystallite size was about 10 nm. Secondary electron images obtained at various stages of conversion are shown in Figure 17. The hollow, cylindrical shape of the *Aulacoseira* frustules was preserved after conversion into SiC. A transmission electron microscope image of a cross-section of a SiC-converted frustule, and an associated electron diffraction pattern, are shown in Figure 18. The dark field image in Figure 18a confirmed the presence of very fine nanocrystals (consistent with XRD analyses). The electron diffraction pattern in Figure 18b revealed the presence of SiC but not Si, which indicated that the 1200°C/12 h treatment was sufficient to allow for complete reaction of the carbon coating with the underlying silicon.

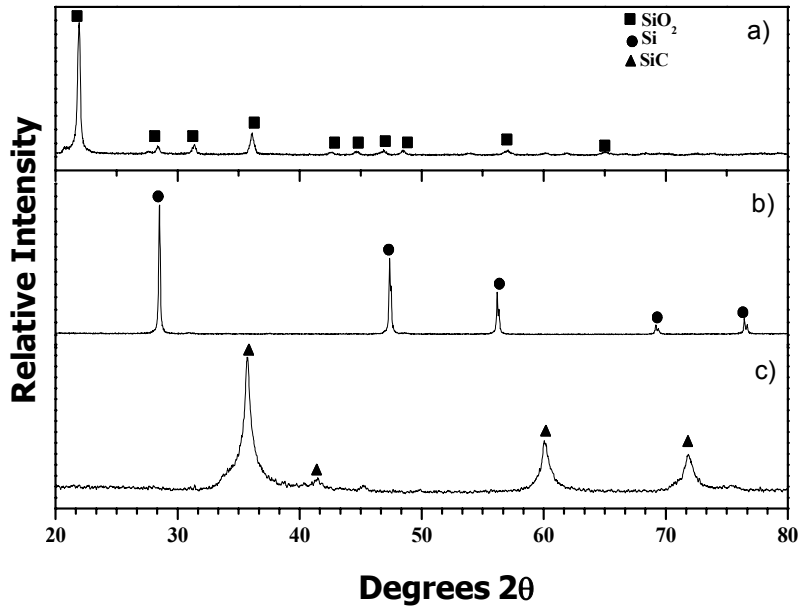

Figure 16. X-ray diffraction patterns of: (a) SiO_2 *Aulacoseira* frustules before reaction, (b) Si replicas of the *Aulacoseira* frustules obtained by magnesiothermic reduction of the silica and then selective dissolution of the MgO product in an aqueous HCl solution, and (c) SiC frustule replicas produced by gas-phase deposition of carbon onto the silicon replicas and then reaction of the carbon with the underlying silicon at 1200°C for 12 h.

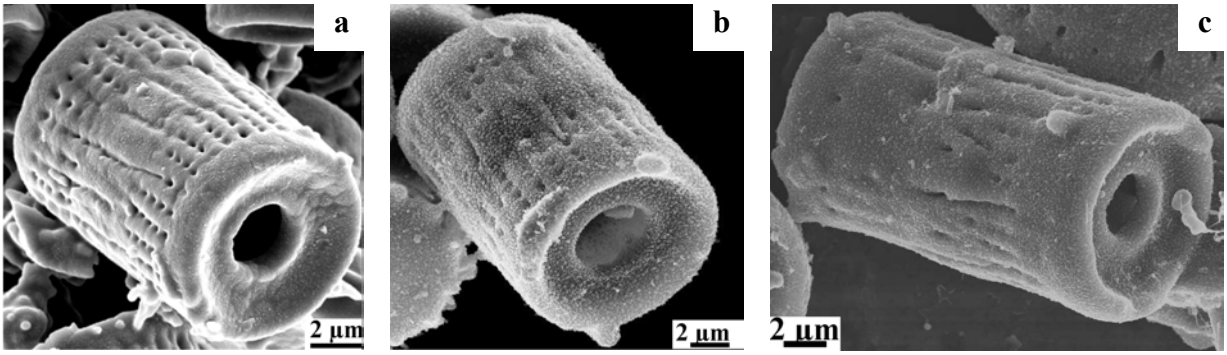

Figure 17. Scanning electron images of : (a) SiO_2 *Aulacoseira* frustules before reaction, (b) Si replicas of the *Aulacoseira* frustules obtained by magnesiothermic reduction of the silica and then selective dissolution of the MgO product in an aqueous HCl solution, and (c) SiC frustule replicas produced by gas-phase deposition of carbon onto the silicon replicas and then reaction of the carbon with the underlying silicon at 1200°C for 12 h.

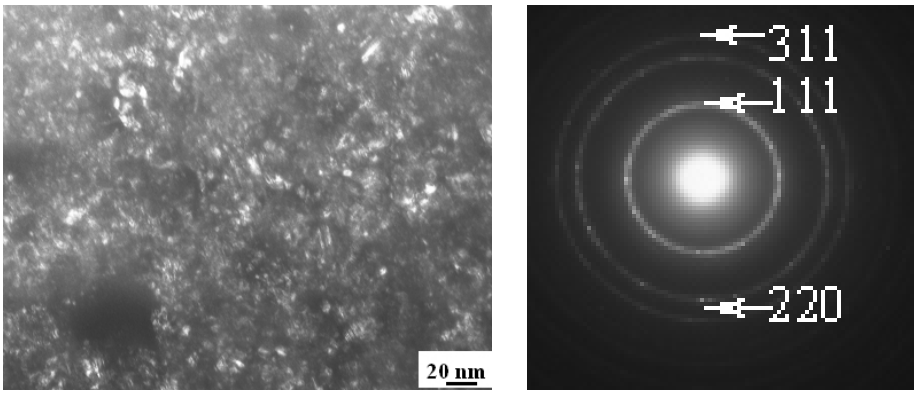

Figure 18. (a) Transmission electron image and (b) selected area electron diffraction pattern obtained from a cross-section of an *Aulacoseira* frustule after conversion into SiC via gas-phase deposition of carbon onto silicon replicas and then reaction of the carbon with the underlying silicon at 1200°C for 12 h.

Chemical Conversion of SiC Replicas of Diatom Frustules into C Replicas of High Surface Area (K. H. Sandhage Group, Georgia Tech)

Porous carbon structures are utilized as chemically inert substrates for a wide variety of applications in catalysis and filtration. The syntheses of open porous carbon particles with well-controlled hierarchical pore structures (i.e., with pore sizes spanning the micrometer to nanometer scales), very high surface areas, and selectable 3-D morphologies, remains a significant challenge.

Over the past year, the conversion of SiC replicas of diatom frustules into C replicas has been examined. SiC frustule replicas were exposed to flowing $Cl_2(g)$ at 950°C for 3 h to allow for selective silicon removal via the following reaction.[9,10]

$$SiC(s) + 2Cl_2(g) => C(s) + SiCl_4(g) \quad (3)$$

Secondary electron images of the resulting carbon-converted diatom frustules, and an associated energy-dispersive x-ray (EDX) analysis, are shown in Figure 19. The cylindrical morphology of

the *Aulacoseira* frustules (Figure 19a) and the disk-shaped morphology of *Cyclotella costei* frustules (Figure 19b) were preserved after conversion into carbon. The EDX pattern shown in Figure 19c confirmed that the silicon had been completely removed via the chlorine treatment at 950°C for 3 h. A transmission electron image of an ion-milled cross-section of a carbon-converted *Aulacoseira* frustule, and an associated selected area electron diffraction pattern, are shown in Figure 20. The electron diffraction pattern was consistent with amorphous carbon, which, considering the low temperature used for this reaction, was the expected form of carbon (i.e., the graphitization of carbon is typically conducted at much higher temperatures). The absence of diffraction spots/rings for silicon carbide in this and other electron diffraction patterns obtained at various positions throughout the specimen cross-section provided further confirmation that the silicon had been completely removed during the 950°C/3h treatment with flowing chlorine gas.

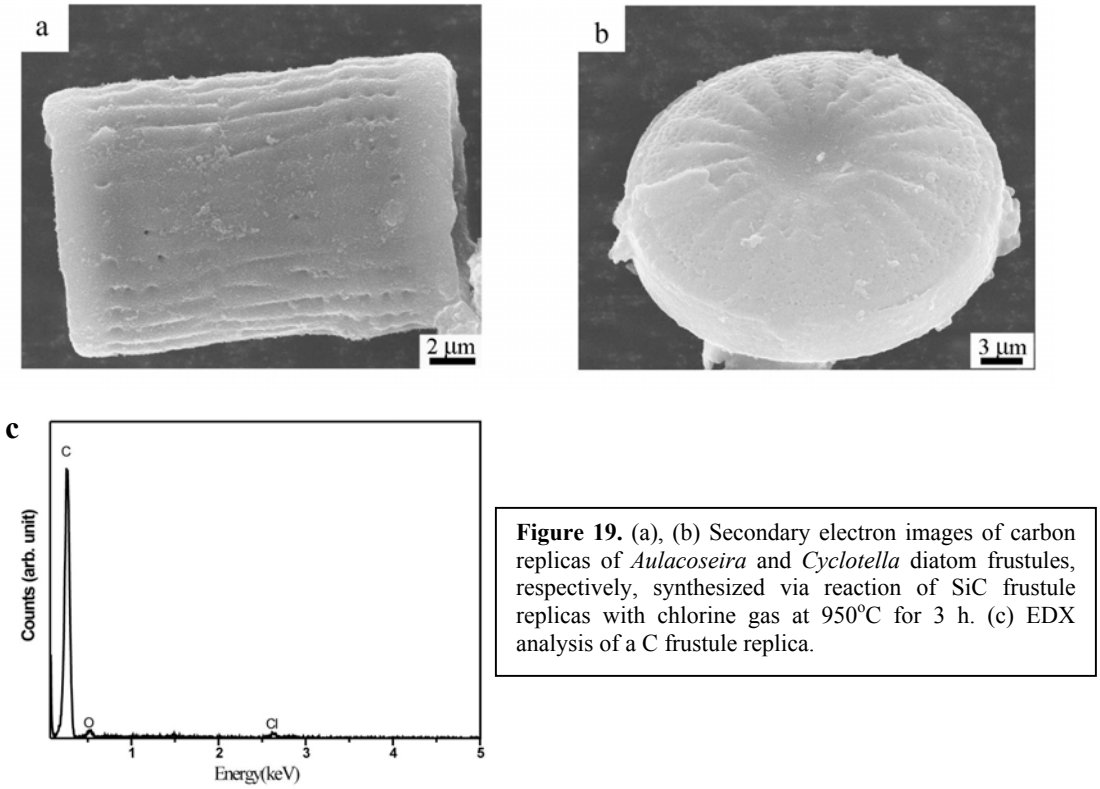

Figure 19. (a), (b) Secondary electron images of carbon replicas of *Aulacoseira* and *Cyclotella* diatom frustules, respectively, synthesized via reaction of SiC frustule replicas with chlorine gas at 950°C for 3 h. (c) EDX analysis of a C frustule replica.

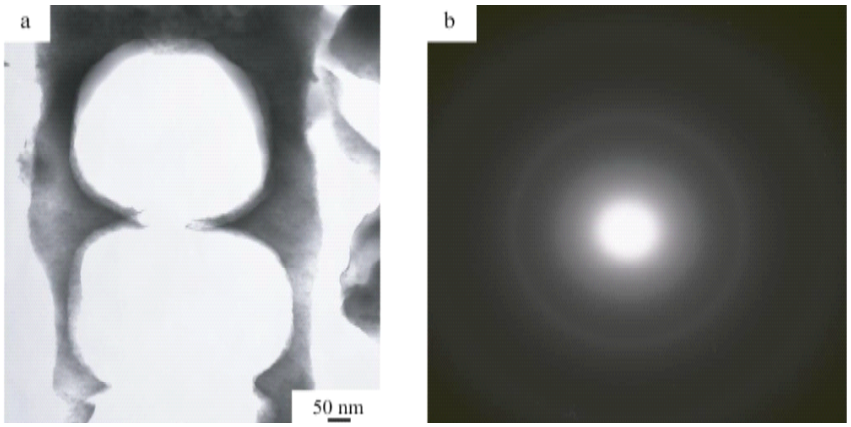

Figure 20. (a) Low magnification bright field transmission electron image of a cross-section of a C replica of an *Aulacoseira* diatom frustule. (b) Selected area electron diffraction pattern obtained from the C replica.

The decrease in solid volume upon conversion of SiC into C was expected to yield carbon replicas with substantial internal porosity. The porosity of the carbon replicas was examined via nitrogen adsorption/desorption analyses. Nitrogen adsorption/desorption curves obtained from C-converted frustules are shown in Figure 21. The Brunauer-Emmet-Teller (BET) surface area, calculated from the nitrogen adsorption profile of the C-converted frustules, was 1370 m^2/g! The C frustule replicas also contained a significant fraction of microporosity. The volume occupied by micropores (i.e., pores $\leq$ 2 nm) was calculated to be 22% of the total volume occupied by pores $\leq$ 36 nm in size.

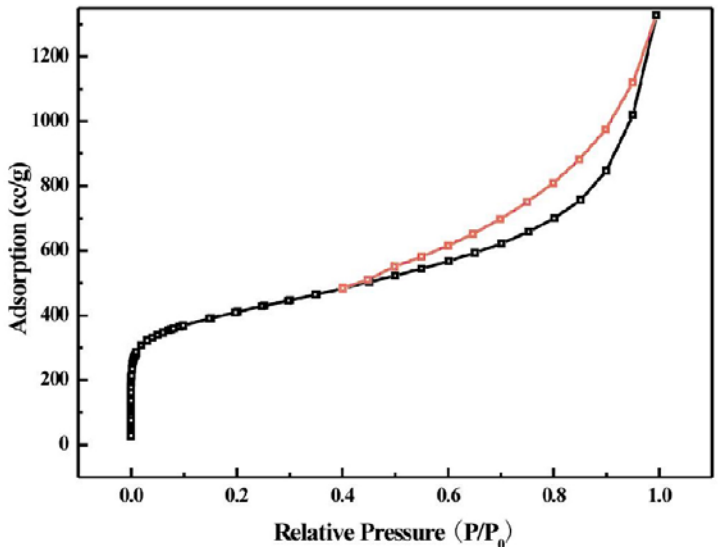

Figure 21. Isothermal (77K) nitrogen adsorption/desorption analyses obtained from C replicas of diatom frustules.

Conversion of Si Replicas of Diatom Frustules into Porous Ag, Au, and Pd Replicas

(K. H. Sandhage Group, Georgia Tech)

A two-step process was developed to convert silica diatom frustules into porous metal replicas: i) conversion of the silica frustules into porous silicon replicas (via the magnesiothermic reduction process described above), and then ii) electroless deposition of noble metals into/onto the porous silicon surfaces, followed by selective dissolution of the silicon template.

The electronic and chemical (reducing) nature of the silicon replica templates[11], relative to the starting silica frustules, enabled the electroless deposition of silver onto the exposed silicon replica surfaces. Silver was deposited onto/into the porous 3-D silicon frustule replicas by immersing the silicon replicas in a commercial silver electroless plating solution heated to 90ºC (as recommended by the vendor) for 1 min. After removal from the solution by filtration and washing with de-ionized water, the Ag-impregnated specimens were immersed in a heated aqueous NaOH solution for 3 h to remove the silicon templates via selective dissolution. X-ray diffraction analysis (Figure 22) confirmed that the final product was composed solely of silver (that is, the silicon dissolution was completed within 3 h of exposure to the heated NaOH solution). Scherrer analysis of this x-ray diffraction pattern yielded an average crystallite size of 14 nm. As demonstrated by the secondary electron image in Figure 23a, the silver product retained the 3-D cylindrical morphology of the starting *Aulacoseira* diatom frustules. The hollow

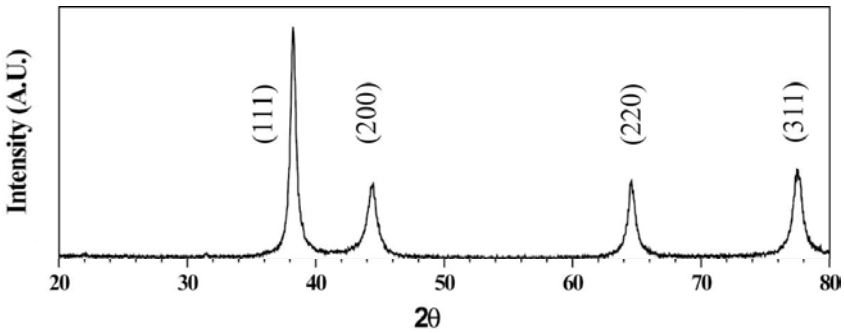

Figure 22. X-ray diffraction patterns obtained from a silver sample generated via electroless silver deposition onto silicon frustule replica templates (synthesized by magnesiothermic reduction of *Aulacoseira* diatom frustules), followed by selective dissolution of the silicon templates. The observed diffraction peaks were consistent with silver (silver (hkl) diffraction planes associated with each peak are indicated).

interior structure of the starting *Aulacoseira* frustule was also preserved in this silver replica, as revealed by the image in Figure 23b that was obtained after ablation of one end of the replica by ion beam milling. A high magnification image of the milled cross-section of the wall of the silver replica (Figure 23c), and an associated energy dispersive x-ray analysis (Figure 23d), indicated that the replica was comprised of a porous network of silver nanoparticles. The continuity of the silver nanoparticles throughout the cross-section of the ion-milled specimen in Figure 23b indicated that the electroless silver solution completely penetrated the pores throughout the walls of the silicon replicas and then deposited on internal particle surfaces of the silicon templates; that is, silver deposition was not localized to just the outside and inside surfaces of the frustule-

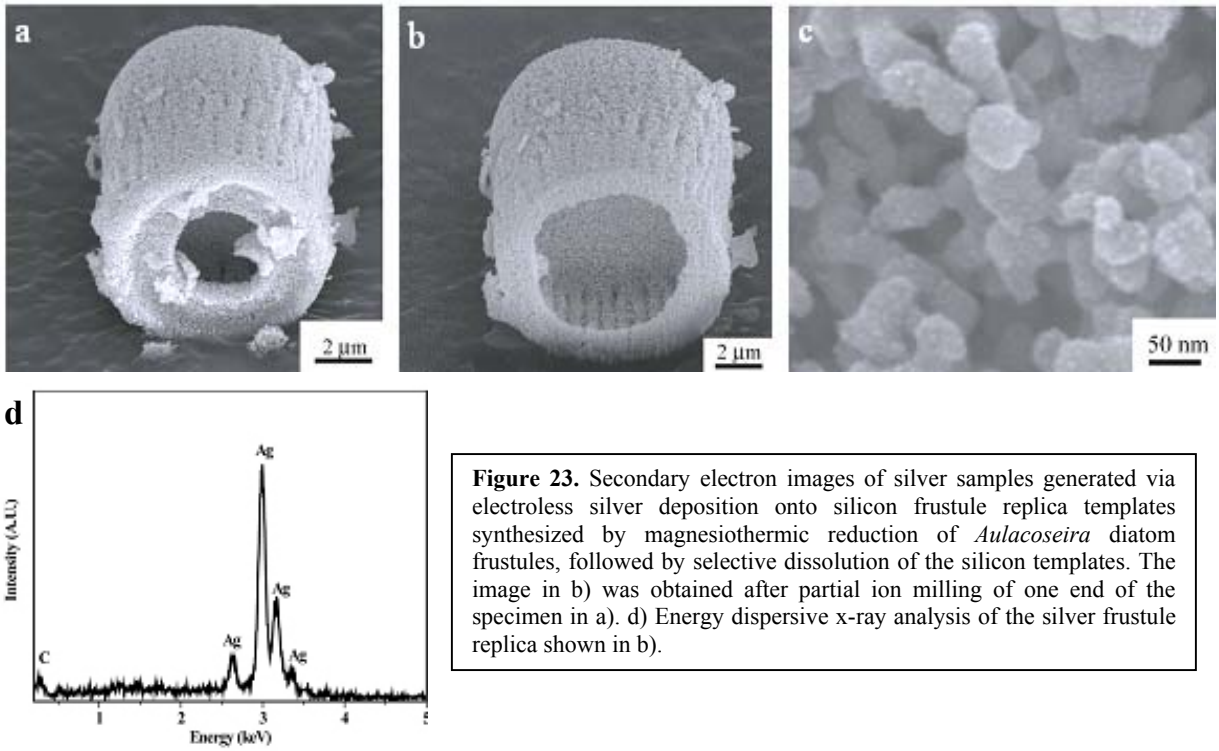

Figure 23. Secondary electron images of silver samples generated via electroless silver deposition onto silicon frustule replica templates synthesized by magnesiothermic reduction of *Aulacoseira* diatom frustules, followed by selective dissolution of the silicon templates. The image in b) was obtained after partial ion milling of one end of the specimen in a). d) Energy dispersive x-ray analysis of the silver frustule replica shown in b).

shaped silicon templates. The extent of silver migration and deposition throughout the walls of the porous silicon replicas was sufficient as to provide silver networks with enough rigidity to allow for preservation of the 3-D silicon frustule replica shape upon the subsequent dissolution of the silicon. The appreciable extent of silver deposition in the pores of the silicon replicas was also revealed by a significant reduction in the measured specific surface area, from 541 to 22.8 m^2/g, after silver deposition and silicon dissolution.

To demonstrate that this approach is not limited to the syntheses of porous 3-D silver nanoparticle structures, gold and palladium frustule replicas were also generated. Silicon frustule replicas were immersed in a commercial gold or a palladium electroless solution[12] heated to 60ºC (as directed by the vendor or reference 18) for 1 min. After removal from the solution by filtration and washing with de-ionized water, the Au- and Pd-impregnated specimens were immersed in a heated, aqueous NaOH solution for 3 h to remove the silicon templates via selective dissolution. X-ray diffraction analyses (Figures 24a, b) confirmed that the final products were composed solely of gold or palladium. The secondary electron images in Figure

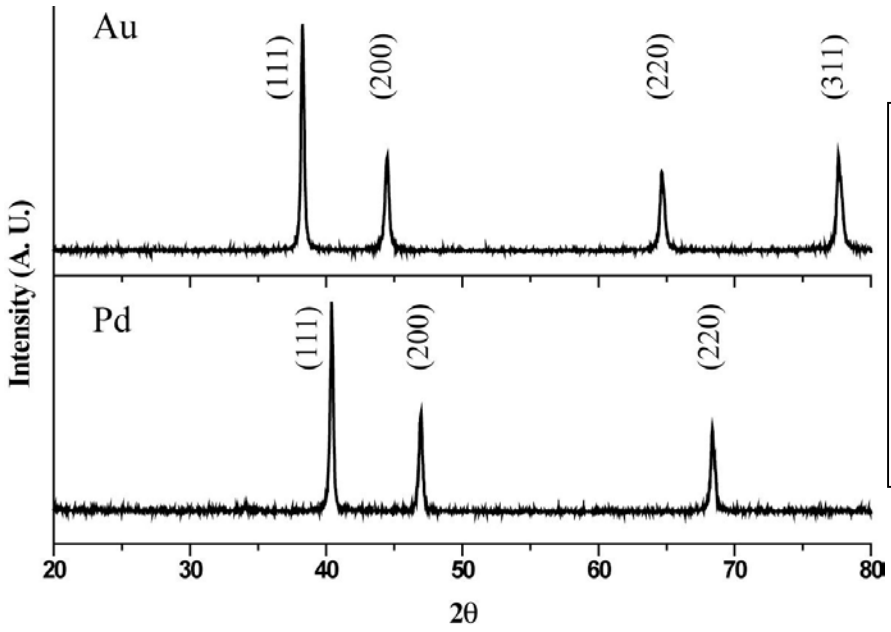

Figure 24. X-ray diffraction patterns obtained from a) Au frustule replicas and b) Pd frustule replicas synthesized via electroless deposition onto silicon frustule replica templates. The observed diffraction peaks were consistent with gold or palladium (gold or palladium (hkl) diffraction planes associated with each peak are indicated).

25 indicate that the gold and palladium products generated from the silicon frustule replicas retained the 3-D cylindrical morphology of the starting *Aulacoseira* diatom frustules. High magnification images of the gold and palladium replicas (Figures 25b, e), and associated energy dispersive x-ray analyses (Figures 25c, f), indicated that the replicas were comprised of porous, interconnected networks of gold and palladium nanoparticles. Scherrer analyses of the x-ray diffraction patterns in Figure 24 yielded average crystallite sizes of 50 nm and 43 nm for the gold and palladium specimens, respectively. BET analyses of nitrogen adsorption measurements yielded specific surface areas of 10.1 m^2/g and 13.3 m^2/g for the gold and palladium frustule replicas, respectively. As for the silver replicas, these values of specific surface area were significantly higher than for the starting *Aulacoseira* frustules (1.7 m^2/g).

This work demonstrates for the first time how freestanding porous 3-D microscale assemblies of noble metal (silver, gold, palladium) nanoparticles with well-controlled and selectable morphologies inherited from (bio)silica templates (diatom frustules) may be synthesized via a combination of gas/solid reaction and wet chemical methods. This scalable process may be used

to generate a variety of porous metal replicas of biologically- or synthetically-derived silica templates with a wide range of 3-D morphologies for use in catalysis, filtration, sensor, electrical, and thermal applications.[13-17]

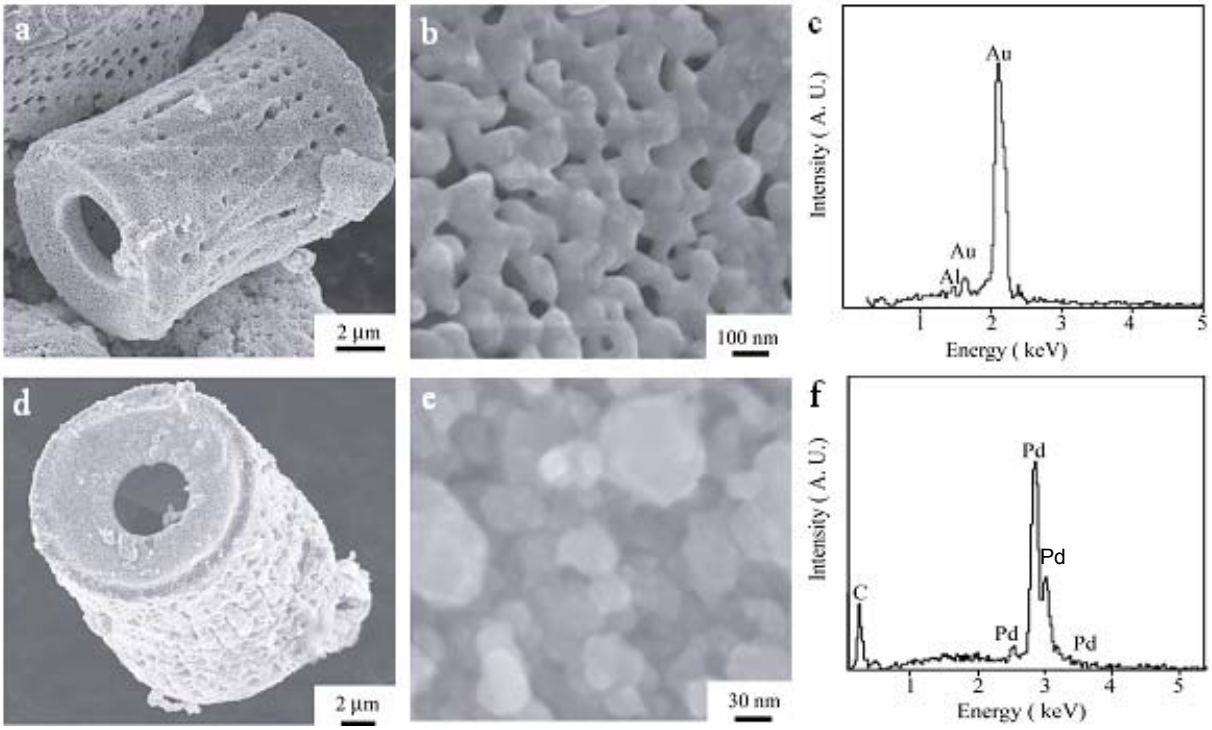

Figure 25. Secondary electron images of a), b) a gold frustule replica and d), e) a palladium frustule replica synthesized via electroless deposition onto silicon frustule replica templates. EDX analyses of the gold and palladium replicas are shown in e) and f), respectively.

References

1. K. M. Ho, C. T. Chan, C. M. Soukoulis, "Existence of a photonic gap in periodic dielectric structures," *Phys. Rev. Lett.* **65**, 3152-3156 (1990).
2. K. M. Ho, C. T. Chan, C. M. Soukoulis, R. Biswas, M. Sigala, "Photonic band gaps in the three dimensions: new layer-by-layer periodic structures," *Solid State Commun.* **89**, 413-416 (1994).
3. R. R. Unocic, F. M. Zalar, P. M. Sarosi, Y. Cai, K. H. Sandhage, "Anatase assemblies from algae: Coupling biological self-assembly of 3-D nanoparticle structures with synthetic reaction chemistry," *Chem. Comm.* [7] 795-796 (2004).
4. S.-J. Lee, S. Shian, C.-H. Huang, K. H. Sandhage, "Rapid, Non-Photocatalytic Destruction of Organophosphorous Esters Induced by Nanostructured Titania-based Replicas of Diatom Microshells," *J. Am. Ceram. Soc.* **90** [5] 1632-1636 (2007).
5. S. R. Hall, H. Bolger, S. Mann, "Morphosynthesis of complex inorganic forms using pollen grain templates," *Chem. Commun.* [6] 2784-2785 (2003).
6. Z. Bao, M. R. Weatherspoon, Y. Cai, S. Shian, P. D. Graham, S. M., G. Ahmad, M. B. Dickerson, B. C. Church, Z. Kang, C. J., H. W. Abernathy, III, M. Liu, K. H. Sandhage, "Shape-preserving Reduction of Silica Micro-Assemblies into Microporous Silicon Replicas," *Nature* **446** [3] 172-175 (2007).

7. *JCPDS X-ray Diffraction Card File*, Card No. 39-1425 for cristobalite SiO_2, No. 27-1402 for Si.
8. H. Tappan, *The Paleobiology of Plant Protists*, W. H. Freeman, San Francisco, CA, p. 572, 1980.
9. S. Welz, M. J. McNallan, Y. Gogotsi, "Carbon structures in silicon carbide derived carbon," *J. Mater. Proc. Techn.* 179 [1-3] 11-22 (2006).
10. Y. Gogotsi, A. Nikitin, H. Ye, W. Zhou, J. E. Fischer, B. Yi, H. C. Foley, M. W. Barsoum, "Nanoporous carbide-derived carbons with tunable pore size," *Nature Mater.* **2** [9], 591-594 (2003).
11. F. A. Harraz, T. Tsuboi, J. Sasano, T. Sakka, Y. H. Ogata, "Metal Deposition onto a Porous Silicon Layer by Immersion Plating from Aqueous and Nonaqueous Solutions," *J. Electrochem. Soc.* **149**, C456-C463 (2002).
12. Z. Shi, S. Wu, J. A. Szpunar, "Self-assembled palladium nanowires by electroless deposition," *Nanotechnol.* **17**, 2161-2166 (2006).
13. V. Zielasek, B. Juergens, C. Schulz, J. Biener, M. M. Biener, A. V. Hamza, M. Baumer, "Gold catalysts: Nanoporous gold foams," *Angew. Chem., Int. Ed.* **45**, 8241-8244 (2006).
14. D. Ding, Z. Chen, "A pyrolytic, carbon-stabilized, nanoporous Pd film for wide-range H_2 sensing," *Adv. Mater.* **19**, 1996 (2007).
15. S. O. Kucheyev, J. R. Hayes, J. Biener, T. Huser, C. E. Talley, A. V. Hamza, "Surface-enhanced Raman scattering on nanoporous Au," *Appl. Phys. Lett.* **89**, 053102/1-053102/3 (2006).
16. R. Zeis, A. Mathur, G. Fritz, J. Lee, J. Erlebacher, "Platinum-plated nanoporous gold: An efficient, low Pt loading electrocatalyst for PEM fuel cells," *J. Power Sources* **165**, 65-72 (2007).
17. R. W. Ertenberg, B. Andraka, Y. Takano, "Prospects of porous gold as a low-temperature heat exchanger for liquid and solid helium," *Phys. B* **284-288**, 2022-2023 (2000).

Personnel:

Faculty:	Prof. Ken H. Sandhage (Georgia Tech)
	Prof. Jennifer A. Lewis (Univ. Illinois)
Post-docs:	Dr. Ye Cai* (Georgia Tech)
	Dr. Bok Yeop Ahn (Univ. Illinois)
Graduate Students:	Mr. Shawn Allan (Georgia Tech); MS degree in MSE; July, 2005
	Mr. Zhihao Bao (Georgia Tech); PhD degree in MSE; December, 2007
	Mr. Samuel Shian (Georgia Tech)
	Mr. Mingjie Xu* (Univ. Illinois); PhD degree in MSE;
	*partially supported by the present AFOSR project

Publications/Accepted or In Print (partially or fully supported by this project, 2005-present):

1. R. F. Shepherd, P. Priyadarshi, Z. Bao, K. H. Sandhage, J. A. Lewis, P. S. Doyle, "Stop-Flow Lithography of Colloidal, Glass, and Silicon Microcomponents," *Adv. Mater.*, accepted, in press.
2. Z. Bao, E. M. Ernst, S. Yoo, K. H. Sandhage, "Syntheses of Porous Self-Supporting Metal Nanoparticle Assemblies with 3-D Morphologies Inherited from Biosilica Templates (Diatom Frustules)," *Adv. Mater.* (for Special Issue on Advanced Biological and Biomimetic Materials Research), accepted, in press.
3. Z. Bao, M. R. Weatherspoon, Y. Cai, S. Shian, P. D. Graham, S. M. Allan, G. Ahmad, M. B. Dickerson, B. C. Church, Z. Kang, C. J. Summers, H. W. Abernathy, III, M. Liu, K. H. Sandhage, "Shape-preserving Reduction of Silica Micro-Assemblies into Microporous Silicon Replicas," *Nature*, 446 [3] 172-175 (2007).
4. S.-J. Lee, S. Shian, Ch.-H. Huang, K. H. Sandhage, "Rapid, Non-Photocatalytic Destruction of Organophosphorous Esters Induced by Nanostructured Titania-based Replicas of Diatom Microshells," *J. Am. Ceram. Soc.*, 90 [5] 1632-1636 (2007).
5. E. M. Ernst, B. C. Church, C. S. Gaddis, R. L. Snyder, K. H. Sandhage, "Enhanced Hydro-thermal Conversion of Surfactant-modified Diatom Microshells into Barium Titanate Replicas," *J. Mater. Res.*, 22 [5] 1121-1127 (2007).
6. K. H. Sandhage, S. M. Allan, M. B. Dickerson, E. M. Ernst, C. S. Gaddis, S. Shian, M. R. Weatherspoon, G. Ahmad, Y. Cai, M. S. Haluska, R. L. Snyder, R. R. Unocic, and F. M. Zalar, "Inorganic Preforms of Biological Origin: Shape-Preserving Reactive Conversion of Biosilica Microshells (Diatoms)," pp. 235-253 in *Handbook of Biomineralization*, Eds. E. Bauerlein, P. Behrens, Vol. 2, Wiley-VCH, Weinheim, Germany, 2007.
7. K. H. Sandhage, "Shaped Microcomponents via Reactive Conversion of Biologically-derived Microtemplates," *U.S. Patent No. 7,204,971*, April 17, 2007.
8. M. Xu and J.A. Lewis, "Phase Behavior and Rheological Properties of Polyamine-rich Complexes for Direct-Write Assembly," *Langmuir* 23 [25] 12752-59 (2007).
9. J. A. Lewis, "Direct Ink Writing of 3D Functional Materials," *Adv. Funct. Mater.,* 16, 2193-2204 *(*2006). *(invited feature cover article)*
10. J. A. Lewis, J. E. Smay, J. Stuecker, J. Cesarano, "Direct-Write Assembly of 3-D Ceramic Structures," *J. Am. Ceram. Soc.,* 89 [12] 3599-609 (2006). *(invited feature cover article)*
11. K. H. Sandhage, S. Shian, C. S. Gaddis, M. R. Weatherspoon, Y. Cai, S. Yoo, M. S. Haluska, R. L. Snyder, Y. Liu, M. Liu, N. Ferrell, D. J. Hansford, M. Hildebrand, B. Palenik,

"Biologically Enabled Syntheses of Nanostructured 3-D Sensor Materials: The Potential for 3-D Genetically Engineered Microdevices (3-D GEMs)," *J. Rare Metal Mater. Eng.*, 35, 13-14, 2006.

12. Y. Cai, M. R. Weatherspoon, E. Ernst, M. S. Haluska, R. L. Snyder, K. H. Sandhage, "3-D Microparticles of $BaTiO_3$ and Zn_2SiO_4 via the Chemical (Sol-Gel, Acetate Precursor, or Hydrothermal) Conversion of Biologically (Diatom) Templates," *Ceram. Eng. Sci. Proc.*, 27 [8] 49-56 (2006).
13. M. Xu, G. M. Gratson, E. B. Duoss, R. F. Shepherd, J. A. Lewis, "Biomimetic Silicification of 3D Polyamine-Rich Scaffolds Assembled by Direct Ink Writing," *Soft Matter*, 2 [3] 205-209 (2006). (Cover Article)
14. S. Shian, Y. Cai, M. R. Weatherspoon, S. M. Allan, K. H. Sandhage, "Three-Dimensional Assemblies of Zirconia Nanocrystals Via Shape-preserving Reactive Conversion of Diatom Microshells," *J. Am. Ceram. Soc.*, 89 [2] 694-698 (2006).
15. M. R. Weatherspoon, M. S. Haluska, Y. Cai, J. S. King, C. J. Summers, R. L. Snyder, K. H. Sandhage, "Phosphor Microparticles of Controlled 3-D Shape from Phytoplankton," *J. Electrochem. Soc.*, 153 [2] H34-H37 (2006).
16. K. H. Sandhage, "Shaped Microcomponents via Reactive Conversion of Biologically-derived Microtemplates," *U.S. Patent No. 7,067,104*, June 27, 2006.
17. M. S. Haluska, I. Dragomir, K. H. Sandhage, R. L. Snyder, "X-ray Diffraction Analyses of 3-D MgO-based Replicas of Diatom Microshells Synthesized by a Low-Temperature Gas/Solid Displacement Reaction," *Powder Diff.*, 20 [4] 306-310 (2005).
18. M. S. Haluska, R. L. Snyder, K. H. Sandhage, S. T. Misture, "A Closed, Heated Reaction Chamber Design for Dynamic High-Temperature X-ray Diffraction Analyses of Gas/Solid Displacement Reactions," *Rev. Sci. Instr.*, 76, 126101-1 - 126101-4 (2005).
19. S. M. Allan, M. R. Weatherspoon, P. D. Graham, Y. Cai, M. S. Haluska, R. L. Snyder, K. H. Sandhage, "Shape-preserving Chemical Conversion of Self-assembled 3-D Bioclastic Micro/nanostructures via Low-temperature Displacement Reactions," *Ceram. Eng. Sci. Proc.*, 26 [3] 289-296 (2005).
20. Y. Cai, S. M. Allan, F. M. Zalar, K. H. Sandhage, "Three-dimensional Magnesia-based Nanocrystal Assemblies via Low-Temperature Magnesiothermic Reaction of Diatom Microshells," *J. Am. Ceram. Soc.*, 88 [7] 2005-2010 (2005).
21. M. B. Dickerson, R. R. Naik, P. M Sarosi, G. Agarwal, M. O. Stone, K. H. Sandhage, "Ceramic Nanoparticle Assemblies with Tailored Shapes and Tailored Chemistries via Biosculpting and Shape-preserving Inorganic Conversion," *J. Nanosci. Nanotech.*, 5 [1], 63-67 (2005).
22. M. R. Weatherspoon, S. M. Allan, E. Hunt, Y. Cai, K. H. Sandhage, "Sol-Gel Synthesis on Self-Replicating Single-Cell Scaffolds: Applying Complex Chemistries to Nature's 3-D Nanostructured Templates," *Chem. Comm.*, [5] 651-653 (2005).
23. M. R. Weatherspoon, S. M. Allan, C. S. Gaddis, Y. Cai, M. S. Haluska, R. L. Snyder, K. H. Sandhage, "Perovskite Particles from Phytoplankton," in *Biological and Bio-Inspired Materials and Devices,* edited by K.H. Sandhage, S. Yang, T. Douglas, A.R. Parker, and E. DiMasi (Mater. Res. Soc. Symp. Proc. 873E, Warrendale, PA , 2005).
24. I. Dragomir-Cernatescu, M. S. Haluska , K. H. Sandhage, and R. L. Snyder, "X-ray Diffraction Analyses of 3-D MgO-based Replicas of Diatom Microshells Synthesized by a Low-Temperature Gas/Solid Displacement Reaction," *Powder Diff.*, 20 [4] 306-310 (2005).

25. K. H. Sandhage, R. L. Snyder, G. Ahmad, S. M. Allan, Y. Cai, M. B. Dickerson, C. S. Gaddis, M. S. Haluska, S. Shian, M. R. Weatherspoon, R. A. Rapp, R. R. Unocic, F. M. Zalar, Y. Zhang, M. Hildebrand, B. P. Palenik, "Merging Biological Self-assembly with Synthetic Chemical Tailoring: The Potential for 3-D Genetically-Engineered Micro/nanodevices (3-D GEMS)," *Int. J. Appl. Ceram. Technol.*, 2 [4] 317-326 (2005).

Interactions/Transitions (partially or fully supported by this project, 2005-2007):

Other interactions include the following technical presentations:

1. S. Shian, S.-J. Lee, C.-H. Huang, K. H. Sandhage, "Rapid Hydrolysis of Pesticides in the Presence of Nanostructured Titania Particles Derived from Diatom Frustules," *Materials Research Society Fall Meeting*, Boston, MA, Nov. 28, 2007.
2. Z. Bao, M. R. Weatherspoon, S. Shian, Y. Cai, P. D. Graham, S. M. Allan, G. Ahmad, M. B. Dickerson, B. C. Church, Z. Kang, H. W. Abernathy, C. J. Summers, M. Liu, K. H. Sandhage, "Chemical Reduction of Complex, Three-Dimensional Silica Micro-Assemblies (Diatom Microshells) into Microporous Silicon Replicas," *Materials Research Society Fall Meeting*, Boston, MA, Nov. 27, 2007.
3. (Invited) K. H. Sandhage, "Bio-Enabled Assembly of Nanostructured Inorganic Materials," *Composites at Lake Louise*, Lake Louise, Canada, Nov. 1, 2007.
4. (Invited, Plenary) J. A. Lewis, "Directed Assembly of Ceramic Films, Granules, and 3D Structures," *Composites at Lake Louise*, Lake Louise, Canada, October 30, 2007.
5. (Invited, Plenary) J. A. Lewis, "Novel Ink Designs for Direct Writing in Three Dimensions," *Society of Rheology*, Salt Lake City, October 10, 2007.
6. (Invited, Plenary) K. H. Sandhage, M. R. Weatherspoon, S. Shian, Z. Bao, E. Ernst, P. Graham, M. B. Dickerson, G. Ahmad, "Biologically Enabled Assembly of Nanostructured Materials with Complex Three-Dimensional Morphologies and Chemistries," *YUCOMAT (Yugoslav Materials Research Society) 2007*, Herceg Novi, Montenegro, Sept. 11, 2007.
7. (Invited) K. H. Sandhage, "Biologically Enabled Processing of Functional Nanostructured Micro-assemblies: The Potential for Three-Dimensional Genetically Engineered Materials and Micro/nanodevices (3-D GEMs)," *Gordon Research Conference on Solid State Studies in Ceramics*, Andover, NH, Aug. 9, 2007.
8. (Invited, Plenary Talk) K. H. Sandhage, "Biologically Assisted Processing of Electroceramics: The Potential for 3-D Genetically Engineered Materials and Micro/nano-devices (3-D GEMs)," *International Conference on Electroceramics (ICE-2007)*, Arusha, Tanzania, July 31, 2007.
9. J. A. Lewis, "Direct-Write Assembly of 3-D Micro-Periodic Structures," *Grace Hopper Lecture*, University of Pennsylvania, April 19, 2007. (invited talk)
10. (Invited) K. H. Sandhage, S. Shian, M. R. Weatherspoon, Z. Bao, P. Graham, D. Lipke, E. M. Ernst, M. B. Dickerson, S. M. Allan, Y. Cai, G. Ahmad, M. S. Haluska, R. L. Snyder, L. M. Sowards, R. R. Naik, "The Bioclastic and Shape-preserving Inorganic Conversion (BaSIC) Route to Chemically Tailored Three-Dimensional Nanostructured Micro-assemblies," *Materials Research Society Spring Meeting*, San Francisco, CA, April 10, 2007.
11. (Invited) J. A. Lewis, "Bio-inspired Mineralization of 3D Polyelectrolyte Scaffolds," (Bio)Polymer-Directed Mineralization Symposium, *American Chemical Society Spring Meeting*, Chicago, IL, March 25-29, 2007.
12. K. H. Sandhage, M. R. Weatherspoon, E. Ernst, Y. Cai, R. L. Snyder, "Multicomponent Particles with Complex and Controlled 3-D Morphologies via Shape-preserving Chemical

Conversion of Diatom Frustule Templates," *31st International. Cocoa Beach Conference and Exposition on Advanced Ceramics and Composites*, Daytona Beach, FL, Jan. 26, 2007.

13. S. Shian, S. Lee, C. Huang, K. H. Sandhage, "Rapid, Non-Photocatalytic Pesticide Hydrolysis in the Presence of Porous Titania Nanoparticle Structures Derived from Diatom Frustules," *31st International Cocoa Beach Conference and Exposition on Advanced Ceramics and Composites*, Daytona Beach, FL, Jan. 26, 2007.
14. (Invited) K. H. Sandhage, "Bio-Enabled Processing of Functional 3-D Nanoparticle Structures: Merging Genetically-Precise, Massively-Parallel Self-Assembly of Natural Micro-organisms with Complex Chemistries from Synthetic Processing," *Colloquium Talk*, Materials Science and Engineering Department, University of Alabama, Tuscaloosa, Nov. 2, 2006.
15. (Invited) K. H. Sandhage, "Precise, Reproducible, and Scalable Fabrication of Functional 3-D Nanoparticle Structures via Biological Assembly and Synthetic Chemical Modification (Devices from Diatoms)," *MS&T Meeting*, Cincinnati, OH, Oct. 19, 2006.
16. J. A. Lewis, "Bio-Inspired Assembly of Complex 3-D Structures," *International Symposium on Bioinspired Synthesis and Materials – From Organic Templates to Functional Nanoscalic Structures*, Max Planck Institute, Schloss Ringberg, Germany, October 12, 2006. (invited talk).
17. (Invited) K. H. Sandhage, "Manufacturing with Micro-organisms," *Ringberg-Symposium on Bioinspired Synthesis and Materials – From Organic Templates to Functional Nanoscalic Structures*, Max Planck Institute, Schloss Ringberg, Lake Tegernsee, Germany, Oct. 12, 2006.
18. (Invited) K. H. Sandhage, "Manufacturing with Micro-organisms," *Colloquium Talk to the School of Civil and Environmental Engineering*, Georgia Institute of Technology, Atlanta, GA, Sept. 21, 2006.
19. (Invited) K. H. Sandhage, S. Shian, M. R. Weatherspoon, P. D. Graham, S. M. Allan, C. S. Gaddis, M. B. Dickerson, Y. Cai, M. S. Haluska, G. Ahmad, B. C. Church, Y. Zhang, and R. L. Snyder, "Mullite Micro-assemblies with Multifarious Morphologies from Micro-algae," *Mullite 2006*, Vienna, Austria, June 12, 2006.
20. (Invited) K. H. Sandhage, S. Shian, M. R. Weatherspoon, P. D. Graham, S. M. Allan, C. S. Gaddis, M. B. Dickerson, Y. Cai, M. Haluska, G. Ahmad, B. C. Church, Y. Zhang, R. L. Snyder, N. Kroger, R. R. Naik, D. Landry, B. P. Palenik, and M. Hildebrand, "Manufacturing with Micro-organisms: Functional 3-D Nanostructures via Biological Assembly and Synthetic Chemical Conversion," *11th International Ceramics Conference (CIMTEC)*, Acireale, Sicily, June 9, 2006.
21. (Invited) K. H. Sandhage, "Functional 3-D Nanostructured Micro-assemblies via Chemical Conversion of Biological Templates: Devices from Diatoms," *Colloquium Talk,* Weapons and Materials Research Directorate, Army Research Laboratory, Aberdeen Proving Grounds, Aberdeen, MD, May 9, 2006.
22. (Invited) J. A. Lewis, "Novel Inks for Direct Writing of 3D Periodic Structures," *Colloquium Talk*, University of California at Berkeley, April, 2006.
23. (Invited) J. A. Lewis, "Direct-Write Assembly of 3-D Micro-Periodic Structures," *Colloquium Talk*, University of Wisconsin at Madison, April, 2006.
24. (Invited) K. H. Sandhage, "Manufacturing with Micro-organisms: Merging Biological Self-Assembly with Synthetic Chemistry to Yield Functional 3-D Nanoparticle Structures,"

Colloquium Talk, School of Materials Science and Engineering, Nanyang Technological University, Singapore, March 23, 2006.

25. (Invited) K. H. Sandhage, "Functional 3-D Nanostructured Micro-assemblies via Chemical Conversion of Biological Templates," *Army Materials Summit*, Gettysburg, PA, March 14, 2006.
26. (Invited) K. H. Sandhage, S. Shian, M. R. Weatherspoon, S. M. Allan, Y. Cai, C. S. Gaddis, P. D. Graham, M. Haluska, G. Ahmad, B. C. Church, R. L. Snyder, M. Hildebrand, B. P. Palenik, and D. Landry, "Manufacturing with Micro-organisms: A New Biological/Synthetic Chemical Paradigm for the Mass Production of Functional 3-D Nanoparticle Structures," *135th Annual TMS Meeting*, San Antonio, TX, March 13, 2006.
27. Y. Cai, M. R. Weatherspoon, M. S. Haluska, R. L. Snyder, and K. H. Sandhage, "3-D Nanocrystal Assemblies of Multicomponent Oxides with Complex, but Biologically-Replicable Shapes," *30th International Conference and Exposition on Advanced Ceramics and Composites*, Cocoa Beach, FL, Jan. 26, 2006.
28. (Invited, Plenary) J. A. Lewis, "Directed Assembly of Patterned Ceramic Films, Granules, and 3D Structures," *9th International Conference on Ceramic Processing Science*, Coral Springs, FL, January, 2006.
29. (Invited) K. H. Sandhage, "3-D Ordered Assemblies of Ceramic Nanocrystals with Biologically-replicable Shapes and with Functional Synthetic Chemistries via the BaSIC Process," *9th International Ceramic Processing Science Symposium*, Coral Springs, FL, Jan. 9, 2006.
30. S. Shian, Y. Cai, S. M. Allan, M. R. Weatherspoon, and K. H. Sandhage, "Synthesis of Nanostructured Ceramic Microparticles with Selectable Intricate 3-D Shapes and Tailored Chemistries via Bioclastic and Shape-preserving Inorganic Conversion (BaSIC)," *9th International Ceramic Processing Science Symposium*, Coral Springs, FL, Jan. 9, 2006.
31. (Invited) K. H. Sandhage, R. L. Snyder, R. R. Naik, M. Hildebrand, B. P. Palenik, R. A. Rapp, D. J. Hansford, and A. T. Conlisk, "Manufacturing with Micro-organisms," 2005 *International Chemical Congress of Pacific Basin Societies (Pacifichem)*, Honolulu, HI, Dec. 18, 2005.
32. (Invited, Plenary) K. H. Sandhage, S. Shian, C. S. Gaddis, M. R. Weatherspoon, Y. Cai, S. Yoo, M. S. Haluska, R. L. Snyder, Y. Liu, M. Liu, N. Ferrell, D. J. Hansford, M. Hildebrand, and B. P. Palenik, "Biologically Enabled Syntheses of Nanostructured 3-D Sensor Materials: The Potential for 3-D Genetically Engineered Microdevices (3-D GEMs)," *6th East Asia Conference on Chemical Sensors*, Guilin, China, Nov. 6, 2005.
33. (Invited) K. H. Sandhage, S. Shian, M. R. Weatherspoon, P. D. Graham, S. M. Allan, C. S. Gaddis, M. B. Dickerson, Y. Cai, M. Haluska, G. Ahmad, B. Church, Y. Zhang, R. L. Snyder, R. R. Naik, D. Landry, B. P. Palenik, and M. Hildebrand, "Manufacturing with Micro-organisms: A Combined Biological and Synthetic Chemical Route to Functional 3-D Nanoparticle Assemblies," *Composites at Lake Louise*, Lake Louise, Canada, Nov. 1, 2005.
34. (Invited) J.A. Lewis, "Direct-Write Assembly of 3D Micro-Periodic Structures," *Composites at Lake Louise*, Lake Louise, Canada, October, 2005.
35. (Invited) K. H. Sandhage, "Functional 3-D Nanoparticle Structures from Micro-organisms", *Colloquium Talk*, Oak Ridge National Laboratory, Oak Ridge, TN, Oct. 7, 2005.
36. (Invited) J. A. Lewis, "Novel Inks for Direct Writing in Three Dimensions," *International Conference on Digital Fabrication*, Baltimore, MD, September, 2005.

37. (Invited) J. A. Lewis, "Bio-inspired Assembly of 3-D Polyelectrolyte Scaffolds," *230th National American Chemical Society Meeting*, Washington DC, August 29, 2005.
38. (Invited) J. A. Lewis, "Novel Assembly Routes for Colloidal Films and 3-Dimensional Structures," *Gordon Conference on Solid State Ceramics*, Tilton, NH, July 20, 2005.
39. (Invited) K. H. Sandhage, "Manufacturing with Micro-organisms: Merging Biological Self-assembly with Synthetic Chemistry to Yield Functional 3-D Nanoparticle Structures," *Colloquium Talk*, Sandia National Laboratory, Albuquerque, NM, July 20, 2005.
40. (Invited) J. A. Lewis, "Direct Writing in Three Dimensions," DuPont, Wilmington, DE, June, 2005.
41. (Invited) K. H. Sandhage, "Manufacturing with Micro-organisms: Merging Biological Self-assembly with Synthetic Chemistry to Yield Functional 3-D Nanoparticle Structures," *79th ACS Colloid and Surface Science Symposium*, Potsdam, NY, June 13, 2005.
42. (Invited) J. A. Lewis, "Nanoparticle Haloing: A New Colloidal Stabilization Mechanism", *Hospira*, Chicago, IL, April, 2005.
43. ((Invited) K. H. Sandhage, R. L. Snyder, R. R. Naik, D. J. Hansford, R. A. Rapp, A. T. Conlisk, M. Hildebrand, B. P. Palenik, "Merging Biological Protein-mediated Self-assembly of Nanoparticle Structures with Synthetic Chemical Tailoring: The Potential for 3-D Genetically-Engineered Microdevices (3-D GEMs)," *2nd World Congress on Industrial Biotechnology and Bioprocessing*, Orlando, FL, April 21, 2005.
44. S. Shian, D. Landry, Y. Cao, B. P. Palenik, M. Hildebrand, K. H. Sandhage, "Chemically-tailored Nanofibers Derived from Self-Assembled Natural Templates," *Materials Research Society Spring Meeting*, San Francisco, CA, March 29, 2005.
45. (Invited) K. H. Sandhage, "Manufacturing with Micro-organisms," *Colloquium Talk*, Institute for Bioengineering and Biosciences, Georgia Institute of Technology, March 17, 2005.
46. (Invited) J. A. Lewis, "Novel Inks for Direct Writing in Three Dimensions," *NSF Advance Lecturer*, Case Western Reserve University, Cleveland, OH, March, 2005.

New Discoveries, Inventions, or Patent Disclosures (2005-2007):

1. Z.-H. Bao, K. H. Sandhage, "Methods for Fabricating Elemental, Alloyed, and Compound Nano-to-Microscale Structures and Nano-to-Microscale Devices via Reactive Conversion and Selective Phase Removal of Nano-to-Microscale Templates, and Nano-to-Microscale Structures and Nano-to-Microscale Devices Made Thereby," *U.S. Patent Application*, submitted Aug. 13, 2007.

Honors/Awards (2005-2007):

- J. A. Lewis, *Fellow, The American Physical Society*, 2007.
- *Plenary Talk*, J. A. Lewis, "Directed Assembly of Ceramic Films, Granules, and 3D Structures," Composites at Lake Louise, Canada, October 30, 2007.
- *Plenary Talk*, J. A. Lewis, "Novel Ink Designs for Direct Writing in Three Dimensions," Society of Rheology, Salt Lake City, October 10, 2007.
- *Plenary Talk*, K. H. Sandhage, M. R. Weatherspoon, S. Shian, Z. Bao, E. Ernst, P. Graham, M. B. Dickerson, G. Ahmad, "Biologically Enabled Assembly of Nanostructured Materials with Complex Three-Dimensional Morphologies and Chemistries," YUCOMAT (Yugoslav Materials Research Society) 2007, Herceg Novi, Montenegro, September 11, 2007.

- *Plenary Talk*, K. H. Sandhage, "Biologically Assisted Processing of Electroceramics: The Potential for 3-D Genetically Engineered Materials and Micro/nanodevices (3-D GEMs)," International Conference on Electroceramics (ICE-2007), Arusha, Tanzania, July 31, 2007.
- K. H. Sandhage, selected as a member of the *National Materials Advisory Board of The National Academies*, 2006.
- *Featured Public Lecture*, J. A. Lewis, Boulder School for Condensed Matter and Materials Physics, 2006.
- *Plenary Talk*, J. A. Lewis, 9th International Conference on Ceramic Processing Science, Coral Springs, FL, January, 2006.
- *Best Paper Award* (2^{nd} Place) for the paper "3-D Microparticles of $BaTiO_3$ and Zn_2SiO_4 via the Chemical (Sol-Gel, Acetate Precursor, or Hydrothermal) Conversion of Biologically (Diatom) Templates," by Y. Cai, M. R. Weatherspoon, E. Ernst, M. S. Haluska, R. L. Snyder, and K. H. Sandhage, 30^{th} International Conference on Advanced Ceramics & Composites, The American Ceramic Society, 2006.
- *Plenary Talk*, K. H. Sandhage, 6^{th} East Asia Conference on Chemical Sensors, Guilin, China, November, 2005.
- J. A. Lewis, *Fellow, The American Ceramic Society*, 2005.
- K. H. Sandhage, *B. Mifflin Hood Professor*, Georgia Tech, 2005